frontiers in Energy Research

REVIEW
published: 09 September 2020
doi: 10.3389/fenrg.2020.00208

Processing, Carbonization, and Characterization of Lignin Based Electrospun Carbon Fibers: A Review

Vida Poursorkhabi[1,2], Mohamed A. Abdelwahab[1,2†], Manjusri Misra[1,2], Hamdy Khalil[3], Bahram Gharabaghi[1] and Amar K. Mohanty[1,2]*

[1] School of Engineering, University of Guelph, Guelph, ON, Canada, [2] Bioproducts Discovery and Development Center, Department of Plant Agriculture, University of Guelph, Guelph, ON, Canada, [3] The Woodbridge Group, Woodbridge, ON, Canada

Greenhouse gas emissions and environmental impacts of petroleum-based fuels and materials have necessitated the development of renewable resource-based alternatives. In the process to extract cellulose for converting it to bioethanol (bio-based gasoline) large quantities of lignin are produced as the main byproduct-making it useful for further processing application for sustainable materials. Lignin is the second abundant source of renewable carbon with an aromatic structure which makes it a potential candidate for carbon fiber production. Since lignin can be dissolved in a variety of organic and non-organic solvents, electrospinning has been used to produce precursor fibers for carbon nanofiber production. These carbon nanofibers have been tested as a potentially sustainable alternative for the current non-renewable electrodes in energy storage and conversion devices such as supercapacitors. Using lignin by-products from the fuel energy sector in making devices for electrical energy sector provides a great opportunity for promoting a circular economy from sustainable materials while also contributing to researching alternative sustainable materials in light of a global pandemic. This review presents a summary of the processing conditions for electrospinning different varieties of lignin, characterization of the electrospun fibers and the carbonization conditions for converting fibers. Different techniques that of the structural properties of the precursor fibers, characteristics of carbon nanofibers and their performance in energy storage devices are discussed. Compared to the other published reviews in this field, this review aims to present the current knowledge on material-processing-lignin-carbon fibers properties relationship.

Keywords: electrospinning, lignin, carbon fiber, fiber properties, heat treatment

OPEN ACCESS

Edited by:
Ashutosh Mittal, National Renewable Energy Laboratory (DOE), United States

Reviewed by:
Yunqiao Pu, Oak Ridge National Laboratory (DOE), United States
Muzaffer A. Karaaslan, The University of British Columbia, Canada

***Correspondence:**
Manjusri Misra
mmisra@uoguelph.ca

†Mohamed A. Abdelwahab, On leave from the Department of Chemistry, Faculty of Science, Tanta University, Tanta, Egypt

Specialty section:
This article was submitted to Bioenergy and Biofuels, a section of the journal Frontiers in Energy Research

Received: *16 April 2020*
Accepted: *04 August 2020*
Published: *09 September 2020*

Citation:
Poursorkhabi V, Abdelwahab MA, Misra M, Khalil H, Gharabaghi B and Mohanty AK (2020) Processing, Carbonization, and Characterization of Lignin Based Electrospun Carbon Fibers: A Review. Front. Energy Res. 8:208. doi: 10.3389/fenrg.2020.00208

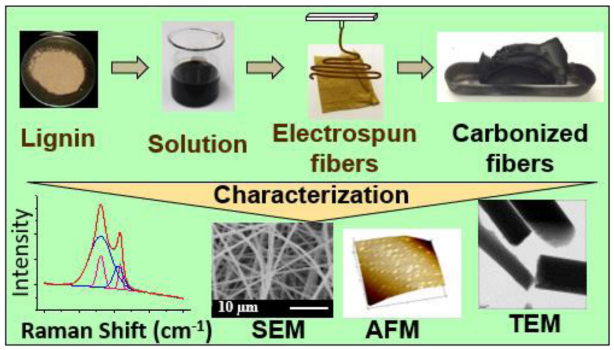

GRAPHICAL ABSTRACT | Electrospun lignin fibers are sustainable and renewable resource-based alternatives to current petroleum-based precursors for carbonized fibers. Production, carbonization, and characterization of lignin fibers are essential for their effective utilization.

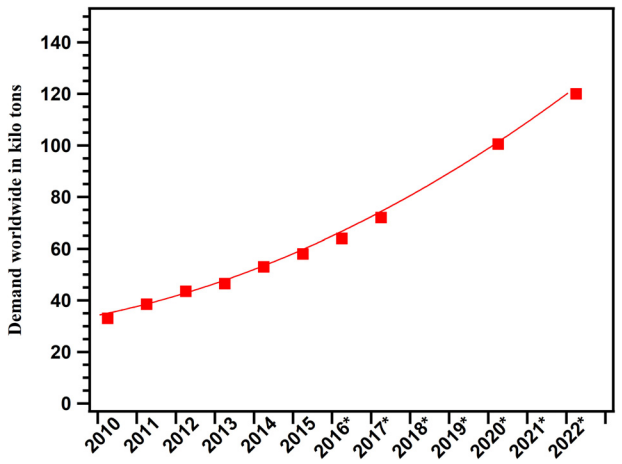

FIGURE 1 | Global demand for carbon fibers in kilo tons from 2010 to 2022. Data adapted from Fang et al. (2017a) with permission from The Royal Society of Chemistry (Order license ID: 1029647-1) (*Estimates).

INTRODUCTION

Environmental institutes set new targets for vehicle engine emissions. Two of the approaches to reach the targeted values are reducing the vehicle weight by using high-performance, lightweight materials and also substituting a fraction of gasoline with bioethanol or other alternative sources of energy (Mainka et al., 2015b; Mohanty et al., 2018).

Addition of bioethanol to gasoline improves the engine performance and reduces emissions (Zhao and Wang, 2020). The economic viability of bioethanol production from sustainable lignocellulosic resources highly depends on the utilization of the process' byproducts for high-value applications. The major byproduct of bioethanol production from lignocellulosic materials is lignin which is one of the most highly available resources of renewable carbon (Solomon et al., 2007; Dessureault, 2014). Compared to cellulose and other sources of renewable carbon, lignin is a good candidate for the production of carbon fibers owing to the aromatic structure, presence of phenolic and aliphatic hydroxyl groups, high carbon content, thermal stability and availability as a waste product from biomass (Fang et al., 2017a).

Advances in the production of efficient energy storage and conversion devices, such as electrodes have led to the emerging utilization of carbon nanofibers. The average annual growth of global carbon fiber is around 58,000 tons in 2015 (**Figure 1**; Fang et al., 2017a). It is estimated that carbon fiber polymer composites will reach 197,000 tons in 2023 (Sauer, 2019). For an economic comparison, current petroleum-based carbon fibers have a high manufacturing cost of ∼USD $10.20 per lb (according to the annual production of 1,500 tons/year (Mainka et al., 2015b; Yoo et al., 2017) whereas utilization of lignin costs ∼USD $ 0.5 per lb, including spinning for the production of carbon fibers which can reduce the cost to ∼USD $2.86 per lb (Fang et al., 2017a). The lower cost of lignin-based carbon fibers provides an opportunity for a wider range of industries to benefit from the advantages of these renewable sustainable fibers. Carbon nanofibers have been used to replace the inorganic components and improve the efficiency and performance of renewable energy storage/conversion devices (Zhang et al., 2016). Several review papers have been published to summarize the research data on electrospinning various types of lignin, their carbonization and properties of the devices fabricated using the carbon nanofibers (Li et al., 2016; Fang et al., 2017a; García-Mateos et al., 2019; Kumar et al., 2019; Wei J. et al., 2019). There are a limited number of comprehensive studies that determine the relationship between the type and properties of lignin – electrospinning process parameters – electrospun fiber properties – carbonization parameters – carbon nanofiber properties, and final performance of the energy storage and conversion devices. The goal of this review is to present a summary of the research reports which describe the materials – processing – performance relationship.

Lignin Structure, Sources, and Applications

Lignin is a heterogeneous, polyaromatic biopolymer comprising ∼30% of organic carbon on the earth (Suhas et al., 2007; Achyuthan et al., 2010; Saito et al., 2012). The lignin content of different biomass varies by type, and it is present in the cell walls of lignocellulosic material (Suhas et al., 2007; Kumar et al., 2009; Laurichesse and Avérous, 2014; Zeng et al., 2014). The monomers and the proposed structure of lignin are represented in **Figure 2**. The lignin monomer structure is attached with different types of bonds and about 48–60% of the inter-unit linkages are β-*O*-4 linkage (aryl-glycerol-β-*O*-4 aryl ether) (Braun et al., 2005).

Softwoods primarily compose of guaiacyl (G) units, with traces of syringyl (S) and p-hydroxyphenyl (H) units present as well. Softwood lignins only have coniferyl alcohol units. Hardwood lignins have both G and S units. Grass or yearly

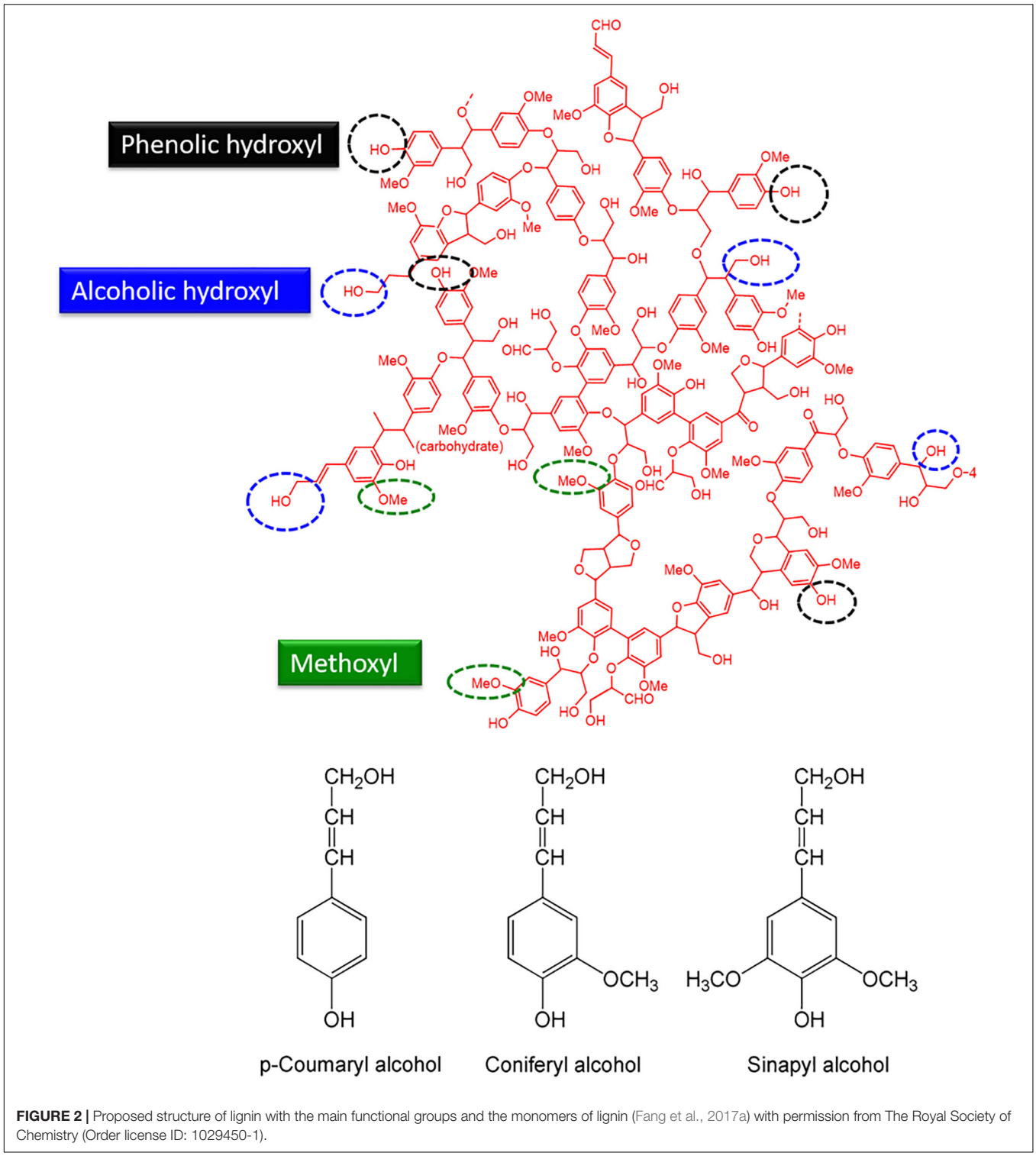

FIGURE 2 | Proposed structure of lignin with the main functional groups and the monomers of lignin (Fang et al., 2017a) with permission from The Royal Society of Chemistry (Order license ID: 1029450-1).

plant lignins have all three units (G, S, and H units) which likely increase economic efficiency in mass production of lignin (Suhas et al., 2007).

Cellulosic ethanol and paper/pulp production are two leading industries that produce lignin as their coproducts (Hu and Hsieh, 2013; Poursorkhabi et al., 2013; Chen et al., 2014; Abdelwahab et al., 2015, 2019; Poursorkhabi et al., 2016; Adams et al., 2018). Alkaline pulping (soda and kraft) are the most common methods to extract lignin from cellulose in paper/pulp manufacturing (Suhas et al., 2007). Paper processes often have high salts and ash content in lignin as well as sulfur-based groups contamination (Lora and Glasser, 2002; Lallave et al., 2007;

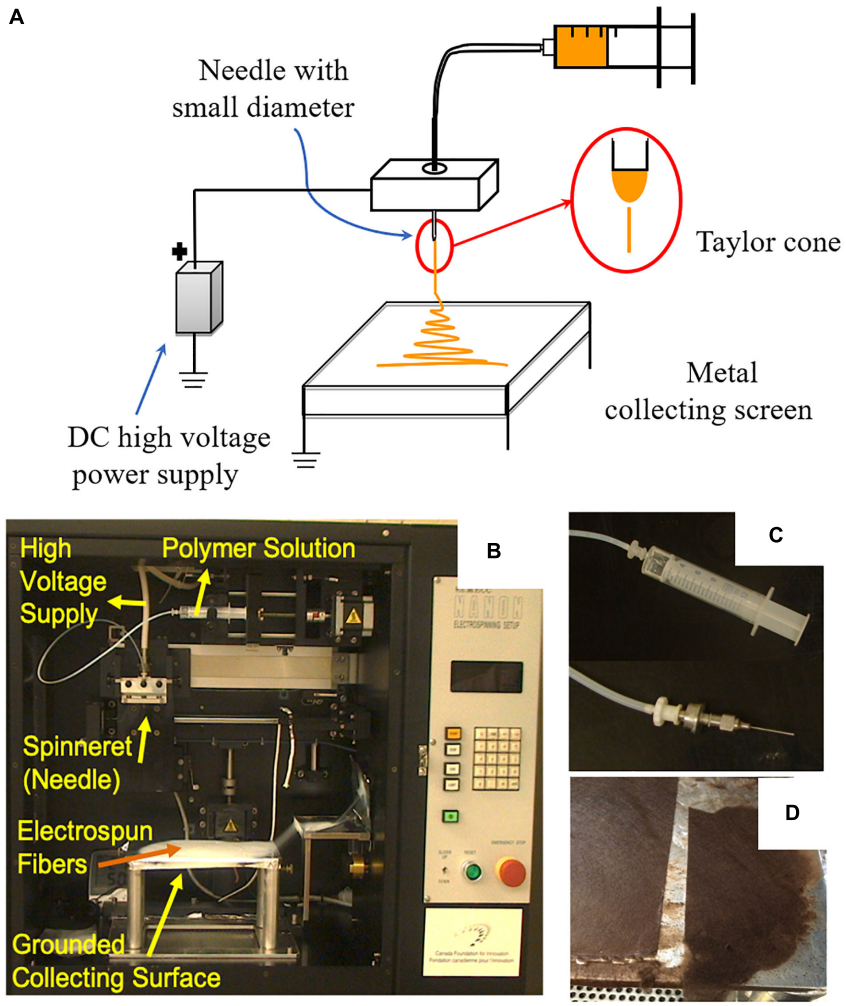

FIGURE 3 | (A) Schematic diagram of electrospinning set up (vertical set-up) reproduced from Poursorkhabi (2016); **(B)** Front view of a commercial electrospinning machine showing the main parts of the process [NANON-01, MECC Co. (Japan)]; **(C)** Needle and syringe connections and **(D)** Sample of collected lignin fibers on a flat collector (**B–D** are original pictures from the Bioproducts Discovery and Development Centre).

Hatakeyama and Hatakeyama, 2010). Biomass conversion technologies use sulfur-free processes. Lignin obtained from these processes has a wide molecular weight distribution and displays different characteristics compared to sulfite and kraft lignin (Lora and Glasser, 2002). The properties of lignins, the extent of hydrolytic degradation, chemical functionalities, and molecular weight depends on the processing conditions and the nature of biomass (Braun et al., 2005; Hu and Hsieh, 2013). Both softwood (Aslanzadeh et al., 2017; Cho et al., 2017, 2018; Roman et al., 2019) and hardwood lignin (Teng et al., 2013; Schreiber et al., 2015; Culebras et al., 2019; Schlee et al., 2019b; Yun et al., 2019) have been used for producing carbon nanofibers. However, most of the literature has studied hardwood lignin. More research is needed to be done to compare the processing and properties of carbon nanofibers obtained from softwood and hardwood lignin under similar processing conditions. Since lignin is produced as a by-product of another industry, i.e., paper and bioethanol, availability of any kind of it is dependent on the economy of these industries. Therefore, the best option is to optimize the production of carbon nanofibers based on the highest available types resulting from the most conventional paper or bioethanol processes.

Electrospinning

Electrospinning process is a convenient and low-cost method to produce continuous fibers (1D structure) at ambient temperatures with micro- to nanometer diameters (Bhardwaj and Kundu, 2010; Inagaki et al., 2012; Poursorkhabi et al., 2016). Nanoparticles (e.g., CuO, NiO, ZnO, etc.) dispersed or embedded in the solution can be incorporated into the polymer to enhance the mechanical and physical characteristics of the matrix providing new advantages for carbon nanofibers in chemical sensing, energy, and catalysis applications (Huang et al., 2003; Tan et al., 2007; Kumar et al., 2012; Xu et al., 2013). In the electrospinning process (**Figure 3**), a polymer solution is placed into a reservoir (syringe), which is attached to a needle in the

top position (vertical set-up) or on the side position (horizontal set-up) of a conductive surface (collector). The spinning begins by charging the needle and pumping the solution that produce drops at the tip of the needle. The Taylor cone (the droplet) gets charged and suctioned into the electrical field between needle and collector, which is grounded. A thin electrified solution jet is suctioned from the droplet when the electrostatic force on the droplet becomes more significant than the surface tension. The jet goes through rapid and unstable whipping motion between the tip and the collector in which the solvent evaporates leaving a fiber material on the collector (Reneker et al., 2000; Ramakrishna et al., 2005; Reneker and Yarin, 2008).

Parameters that affect the electrospinning process and quality of the fibers are material types, processing, environmental conditions, and design. Material properties determine their ability to create fibers. The most important properties in this group are solution viscosity or concentration and molecular weight of the polymer. Higher molecular weight polymers are more suitable for spinning (Deitzel et al., 2001; Li and Wang, 2013). Different processing parameters lead to different geometry, and fiber diameter properties (Thompson et al., 2007; Alghoraibi and Alomari, 2018; Prabu and Dhurai, 2020). The main processing parameters which can be modified include voltage and feeding rate (Teo et al., 2011; Kumar et al., 2012). Increased voltage and decreased feeding rates reduce the fiber diameter (Beachley and Wen, 2009; García-Mateos et al., 2019). Environmental conditions such as temperature and humidity can affect the morphology and the diameter of the fiber (Li and Wang, 2013).

Various designs of electrospinning set-up have been used to increase the throughput of the process or to create different fiber geometries. In needleless setup, the polymer solution is kept in a charged bath and collector is mostly in the shape of a drum rotating on top of the solution bath (Wei L. et al., 2019). During the process, jets of solution emerge from the solution bath and go towards the collector. Another method is co-axial electrospinning where a hollow or core-shell geometry is generated depending on the geometry of the needle (Teo et al., 2011; Persano et al., 2013; Han and Steckl, 2019).

Electrospinning of Lignin

Electrospinning solutions of lignin alone result in electro-spraying of particles because lignin cannot create enough chain entanglements within the solution (Lai et al., 2014b). Multiple approaches used to electrospin lignin include; blending with a second polymer (binder polymer), co-electrospinning, and solvent fractionation to remove the low molecular weight fractions (**Table 1**).

Poly (ethylene oxide) (PEO) is particularly suited polymer to combine with lignin for electrospinning. PEO is miscible with lignin and is water-soluble. A solution of lignin with high molecular weight (M_w) PEO in either alkaline water or organic solvents enhances the spinnability and solution elasticity (Kadla and Kubo, 2003; Kubo and Kadla, 2006; Dallmeyer et al., 2010; Schreiber et al., 2012; Poursorkhabi et al., 2015). A higher concentration of alkali hydroxides in the aqueous solutions of PEO and lignin causes further deterioration in fiber diameter due to improved charge density as well as charge dissipation (Hu and Hsieh, 2013).

Solutions of polyacrylonitrile (PAN) and lignin in DMF (*N,N*-dimethyl formamide) have been electrospun to replace a part of PAN with lignin in the fibers (Seo et al., 2011; Choi et al., 2013). The conductivity and viscosity of PAN-lignin solutions decreased by increasing the lignin concentration (Seo et al., 2011). Thinner fibers were spun from solutions with lower viscosities (Choi et al., 2013). Core-shell fibers were formed by electrospinning cellulose nanofibers as core and PAN/lignin solution as a shell (Xu et al., 2013).

Electrospinning lignin blends with biobased polymers such as cellulose (Ahn et al., 2014), soy protein (Salas et al., 2014), cellulose acetate (Schreiber et al., 2015) and chitosan (Schreiber et al., 2014) have also been reported. Ahn et al. (2014) investigated the electrospinning of lignin and cellulose by direct blending and by partially delignification of hemp fibers to have natural blends of cellulose and different amount of lignin. Salas et al. (2014) investigated the electrospinning of kraft lignin and soy protein in the presence of coadjutant PEO and found an enhancement in the fiber diameter by an increasing amount of lignin and there is a H-bond interaction between lignin and soy protein. Schreiber et al. studied electrospinning of lignin with cellulose acetate (Schreiber et al., 2015) and with chitosan (Schreiber et al., 2014) to improve the carbonization process. They found a good interaction between lignin and cellulose acetate. Lignin/chitosan (in a ratio of 4:3) solution was found to be the best ratio to produce a good fiber due to the balanced charge ratio of lignin and chitosan functional groups.

Polymer blending of lignin with other polymers enhances the characteristics of lignin, however, it will increase the cost of the final product. Hence, retaining the proportion of the polymer binder as low as possible is preferred. Without the addition of an extra polymer (free binder), Lallave et al. (2007) produced co-electrospinning method for spinning lignin (organosolv lignin with low M_w). In the co-electrospinning process, a tri-axial configuration was used. In this configuration, ethanol, lignin solution, and glycerin solution were the outer layer, middle layer, and the inner layer, respectively. Hollow carbon fibers have been produced from co-electrospun fibers.

Production of Carbon Fiber From Lignin-Based Fibers

For producing carbon fibers, a thermostabilization process precedes carbonization. Thermostabilization involves slow air oxidation and cross-linking of the material to raise or remove its thermal transition points. This prohibits the melting of the fibers during carbonization (Braun et al., 2005; Ruiz-Rosas et al., 2010b). There is no melting point for lignin, however, glass transition temperature (T_g) is an important parameter that impacts lignin's mobility and thermal flow. The T_g of lignin and most of the carbon fiber precursors are lower than their thermal decomposition temperature. Therefore, the first processing step is to thermally stabilize the material and prevent fibers softening and fusion prior to the carbonization (Ruiz-Rosas et al., 2010b). The second thermal treatment process,

TABLE 1 | Solution composition and spinning conditions for electrospinning of lignin.

Material			Solution composition		Spinning conditions				References
Lignin type	**Binder polymer**	**Solvent**	**Lignin/Binder polymer (wt/wt%)**	**Total polymer conc. (wt/v%)**	**Voltage (kV)**	**Feed rate (mL/min)**	**Distance (cm)**	**Needle gauge**	
SKL[1], HKL[2], Alcell lignin, SOL[3], Pyrolytic lignin	PEO[4]	DMF[5]	99/1–95/5	20–50	9–14	0.03	14–20	18	Dallmeyer et al., 2010
SulKL[6], LS[7]	PEO[4]	Water	99/1–95/5	10–50	9–14	0.03	14–20	18	Dallmeyer et al., 2010
Alkali Lignin[12]	PAN[8]	DMF[5]	0/100, 50/50, 60/40, 70/30, 80/20	–	15	0.02	10	25.5	Seo et al., 2011
Fractionated SKL[9]	PEO[10]	DMF[5]	Lignin conc.:26–32% PEO conc.: 0.2%	–	15	–	20	22	Dallmeyer et al., 2013, 2014
Fractionated SKL[9]	PEO[10]	DMF[5]	99/1, 1% PEO and 1, 4, 6% MWNTs	25	15	0.03	18	21	Teng et al., 2013
Lignin[11]	PAN[8]	DMF[5]	0/100, 30/70, 50/50	12	15	0.02	10	–	Choi et al., 2013
Organosolv lignin	PEO[4], PAN[8]	DMF[5]	90/10 (99/1 to 80/20)	24	6.5–7	0.017	10	22	Wang et al., 2013
Alkali Lignin[12]	PEO[4]	Water	7.4/2.6, 8.6/1.4, 9/1.Lig./PEO:9/1): 0.1, 0.3, 0.5	10.8 11.7 10	10–15	0.017	12–20	24	Hu and Hsieh, 2013; Hu et al., 2014
Lignin[11]	PVA[13]	Water	30/70, 50/50, 70/30	9–12	26	0.02	25	22	Lai et al., 2014a,b
Lignin[11]	PVA[13]	Water	20, 50, 75% lignin. 5, 10, and 15 wt% CNC added to 20/80 and 75/25.	PVA solution: 5 or 8wt%	19	0.008	22	22	Ago et al., 2012a,b, 2013
Sodium carbonate lignin	Chitosan PEO[14]	Acetic acid, water	0.6% PEO, 1.5% chitosan and 1.5, 2, 2.5, or 3.0% lignin		14	0.002	22.5	24	Schreiber et al., 2014
Hardwood organosolv lignin	Cellulose acetate	Acetone, DMAc[15]	1/1, 2/1, 3/1, 4/1, 5/1	30	16–18	0.01	22.5	24	Schreiber et al., 2015
SKL[1]	PEO[14,16]	DMF[5], NaOH/H_2O	95/5, 97/3	5, 7, 9, 11	20	0.003	22	24	Poursorkhabi et al., 2015
Lignin[11]	PAN[8]	DMF[5]	1/1	15	17	0.002	25	17	Xu et al., 2014

(Continued)

TABLE 1 | Continued

Material			Solution composition		Spinning conditions				References
Lignin type	**Binder polymer**	**Solvent**	**Lignin/Binder polymer (wt/wt%)**	**Total polymer conc. (wt/v%)**	**Voltage (kV)**	**Feed rate (mL/min)**	**Distance (cm)**	**Needle gauge**	
Kraft lignin	PEO[17], soy protein or glycinin,	10 vol-% acetonitrile in 0.1 N NaOH	PEO: 10% of soy: 78, 50, 33, 22	8	15	0.008	22	22	Salas et al., 2014
Lignin-phenol-formaldehyde resin	Polyvinyl-pyrrolidone	DMF[5]	3/1	30	24	0.0065	30	–	Guo et al., 2015
Kraft lignin-g-PAN	–	DMF[5]	–	15–18 wt%	9–11	0.00085–0.0105	15	18	Youe et al., 2015
Hardwood organosolv lignin	PAN[8]	DMF[5]	10/90 to 100/0	18–55	10–15	0.01–0.07	15	21	Oroumei et al., 2015
SKL[1]	PEO[4]	DMF[5]	Lignin: 30 wt% PEO: 0.2 wt%		15	0.03	20	–	Gao et al., 2015
Alkali lignin	PAN[8] PVA[13]	DMF[5]	10 wt% of PAN in DMF, 12 wt% lignin in PVA (lignin/PVA 70/30 wt.%)		16 and 26	0.016–0.02	26	25	Beck et al., 2017
Sulfur-free Softwood Lignin (SFSL)	PEO[10]	DMF[5]	30 wt% in PEO/SFSL/DMF, with PEO/SFSL ratio of 1/99		70×10^3 V/m	4.2×10^{-10} m^3 s^{-1}	20	20	Aslanzadeh et al., 2017
Extracted lignin from corn stalk	PEO[16]	DMF[5]	30 wt% in DMF with a ratio of lignin to PEO as 95:5 wt.%.		20	0.0083	20	20	Shi et al., 2018
Kraft lignin from FP Innovation	PEO[10]	DMF[5]	Lignin/PEO (99/1 w/w), zeolite/lignin = 1–5 wt%		12	0.02	15	18–25	Bahi et al., 2017
Alkali lignin (M_v = 5000-6000)	(PZAA@CNTs)[18], PEO[4]	DMF[5]	Lignin/PEO weight ratio of 96:4 0.5–2 wt% PZAA@CNTs		40	20 μL/min	15	19	Liu et al., 2020
Alkali lignin (AL)	PVA[19]	NaOH/water	15 wt%.PVA, AL in 1M NaOH to 15 wt% AL, 3:7 and 5:5 AL : PVA		10–25	0.00083–0.01	10–20 cm	20	Camiré et al., 2020
Alkali lignin (AL)[13]	PVA[20]	Water	AL: PVA 75:25.		17	0.0083	20	–	Wei J. et al., 2019
Alkali lignin	PVA[21]	Water	Lignin/PVA (10 wt%.)		20	0.08	20	22	Zhang et al., 2019
Fractionation SKL[1]	PEO[22], NCCs	DMF[5]	27 wt.%. lignin, 1 wt.% PEO, 5 wt.% NCC in MF		+20	0.01	20	20	Cho et al., 2019b
fractionation of SKL[1]	PEO[22], NCCs	DMF	25–30 wt.%. lignin, 1 wt.% PEO, 1–5 wt% NCC in DMF		+20	0.01–0.03	20–30	25	Cho et al., 2017
Kraft lignin nanoparticle (KLN) [23]	PVA[21], PGS	75:25 of H_2O and DMF	18% w/v DMF at 40:60 wt.% of PVA-pPGS, 0–5 wt% lignin		19	0.0083	30	21	Saudi et al., 2019

(Continued)

TABLE 1 | Continued

Material			Solution composition		Spinning conditions				References
Lignin type	**Binder polymer**	**Solvent**	**Lignin/Binder polymer (wt/wt%)**	**Total polymer conc. (wt/v%)**	**Voltage (kV)**	**Feed rate (mL/min)**	**Distance (cm)**	**Needle gauge**	
Lignin extracted from cornstalk residues	PAN, GN[24]	DMF[5]	0.05–0.3wt.% GNs, 20 wt.% PAN		15	0.0167	15	–	Dai et al., 2019
Lignin (L)[25]	PLA, TPU, MDI[26]	THF, DMF	L/20–50%PLA+7%MDI in THF/DMF (1:1), L/20–50%TPU+7%MDI in DMF		7.7	30 μL.min^{-1}	10	–	Culebras et al., 2019
Kraft lignin[11]	PAN[8]	DMF[5]	PAN:Lignin 90:10, 80:20 and 70:30 wt.%) in 10% solution		19	0.0133	16	–	Perera Jayawickramage et al., 2019
Alkali lignin	PVA	Acetic acid	10 wt% PVA, Lignin, PVA soln., and acetic acid = 1:1:3 (w/v/v)		18	0.4	–	22	Song et al., 2017, 2019; Meng et al., 2019
Hardwood lignin	Pitch, PAN, zinc acetate	DMF[5], THF	PAN:lignin 9:1, 20 wt% of pitch in THF to achieve PAN/pitch 7/3 wt%. zinc acetate (3, 5, 10 wt.%)		–	–	–	–	Yun et al., 2019
Kraft lignin[11]	rPET[27]	Trifluoroacetic acid	Lignin 20–50%, Conc. (15–25 w/v),		20–30	0.1–2 μL/min	7, 13.5, 20	21	Svinterikos and Zuburtikudis, 2017; Svinterikos et al., 2019
Biorefinery lignin (Protobind 2400)	PAN[28] GRP[29]	DMF[5]	1, 5% GRP, 20 wt.%PAN, Lignin: PAN 50:50, 25:75, 15:85		24	0.005		22	Demiroğlu Mustafov et al., 2019
50 wt% fractionated hardwood Kraft lignin	–	DMF[5]	–		–	0.0166	13	22	Schlee et al., 2019b
Kraft lignin (Indulin AT)	PVA[30]	DMSO	DMSO with conc. 3 to 15 wt%		15–20	0.00833	20	21	Roman et al., 2019
Kraft lignin	PEO[22]	1 M NaOH, $NaNO_3$	10–50 mol% $NaNO_3$/ polymer. PEO/lignin in 1 M NaOH. Polymer was 12 wt%		19–24	0.0166	18, 20	23	Schlee et al., 2019a
Alkali lignin[11]	PVA	Water	Lignin in H_2O then add PVA		26	0.02	25	18	Ma et al., 2019
OL[31]	PAN[8]	DMF[5]	PAN:lignin 10:0, 7:3, 5:5, 3:7 wt.%		–	10 μL min^{-1}	15	20	Dalton et al., 2019
Kraft Lignin (KL)	cellulose acetate (CA)	Acetone, *N,N*-dimethyl cyclohexylamine	KL:CA 1:1 with conc. 8 wt.% in solvent (2:1 v/v).		20	0.0125	20	–	Jia et al., 2018

(Continued)

TABLE 1 | Continued

Material			Solution composition		Spinning conditions				References
Lignin type	**Binder polymer**	**Solvent**	**Lignin/Binder polymer (wt/wt%)**	**Total polymer conc. (wt/v%)**	**Voltage (kV)**	**Feed rate (mL/min)**	**Distance (cm)**	**Needle gauge**	
Lignin[11]	PVA[36]	Water	5 wt% PVA solution		15–20	0.01666	20	22	Zhao et al., 2018
Lignin extracted from Acacia wood powder	PVA[32] $AgNO_3$	Methanol, water	PVA:lignin 9:1 in methanol: H_2O (60:40)		15	10	12	22	Aadil et al., 2018
Solvent fractionated Softwood kraft lignin, Indulin AT	PEO[22]	Water	H_2O at conc. (0.1–0.3 wt%).		25–30	0.01	25	–	Cho et al., 2018
Alkali lignin	PVP[33]	DMF[5]	$Mg(NO_3)_2{\cdot}6H_2O$/lignin 0.5:1, 1:1 and 2:1 wt.%		15	0.0033	15	–	Ma et al., 2018
Lignin containing sulfur	PVA[20] MWNTs [35]	Water	10%PVA, 1 wt.% t-MWNT		25–30	7–10 μL/min	10	21	Lee et al., 2018
Extracted Organosolv and alkaline Lignin	PEO[37]	DMF	Lignin/PEO 30 wt% in DMF with lignin: PEO as 95:5 wt.%.		20	0.00833	20	20	Shi et al., 2018
Alkali Lignin (low sulfonate content)	PAN[8]	DMF	PAN:lignin 12 and 18 wt%, PAN/lignin: 80/20, 50/50		8.5	–	20	–	Lei et al., 2017
Lignin[11]	PVA[13], Surfactant[38]	Water	Lignin: PVA in H_2O, Surfactant mass: 0.2–1.2.		22	0.0166	15	22	Fang et al., 2017b
Lignin[11]	PAN[8]	DMF, Pluronic P123	88 wt% PAN in DMF added to PAN/lignin was 1:1		20	0.025	15	–	Shi et al., 2017

Co – electrospinning

Shell solution	**Core solution**	**Voltage (kV)**	**Feed rate**	**Distance (cm)**	**Needle gauge**	**References**
Ethanol	Alcell lignin/ethanol: 1/1 w/w	12	10% of lignin solution	20–25	–	Lallave et al., 2007
Ethanol	Alcell lignin/ethanol: 1/1 w/w Inner core: glycerine	12	Ethanol/lignin/ glycerine: 0.05/0.5/0.01 to 0.1/1/0.25 mL/h	20–25	–	Lallave et al., 2007
Ethanol	Alcell lignin/ethanol: 45/55 w/w%	12	Ethanol: 0.1 mL/h lignin solution: 1 mL/h	30	–	Berenguer et al., 2015

(Continued)

TABLE 1 | Continued

Material			Solution composition		Spinning conditions				References
Lignin type	**Binder polymer**	**Solvent**	**Lignin/Binder polymer (wt/wt%)**	**Total polymer conc. (wt/v%)**	**Voltage (kV)**	**Feed rate (mL/min)**	**Distance (cm)**	**Needle gauge**	
Ethanol	Lignin/ethanol/platinum acetyl acetonate: 1/1/0.002 and 1/1/0.004 w/w			12	Ethanol: 0.001 mL/min Lignin: 0.014 mL/min		20–25	–	Ruiz-Rosas et al., 2010b
sol–gel Alkoxide	Alcell lignin/Ethanol: 1/1 w/w			Not specified	Core: 0.067 mL/min Shell: 0.008 mL/min		Not specified	–	Ruiz-Rosas et al., 2010a
17% Alkali kraft lignin (Aldrich)/PAN): 1/1	Acetylated cellulose nanofiber/silicone oil/ chloroform mixture			17	Core and shell: 0.03 mL/h		~ 20	Inner:19 Outer: 15	Xu et al., 2013
17% Alkali kraft lignin (Aldrich)/PAN): 1/1	Pure glycerin			17	Core and shell: 0.03 mL/h		~ 20	Inner:19 Outer: 15	Xu et al., 2013
Acetic acid lignin and PEO in DMF, $Fe(Acac)_3$ additive in the shell[34]	35 wt% of SAN[34] dissolved in DMF			25–30	Core: 0.4 mL/h Shell: 1 mL/h		15–20	–	Yu et al., 2018
Ethanol	H_3PO_4/lignin, H_3PO_4(85 wt.%) /lignin /ethanol (0.3/1/1 weight ratio)			24	Core: 3 cm^3 h^{-1} Shell: 0.3 cm^3 h^{-1}		–	30	García-Mateos et al., 2018
Ethanol	1:1 Lignin:ethanol, lignin: ethanol: H_3PO_4 (1:1:0.3), platinum acetylacetonate:lignin 0.006:1 and 0.03:1			14 and 22	Core: 0.0016, 0.005 Shell: 0.0166, 0.05		25	–	García-Mateos et al., 2017

[1]SKL, Softwood kraft lignin (Indulin-AT); [2]HKL, Hardwood kraft lignin; [3]SOL, Softwood organosolv lignin; [4]PEO with M.W. = 600K g/mol; [5]N,N-dimethyl formamide; [6]SulKL, Sulfonated kraft lignin; [7]LS, Lignosulfonate; [8]PAN with M.W. = 150–160K g/mol; [9]Fractionated SKL to a low M.W. fraction (M_w = 6800, M_n = 3000) and a high M.W. fraction (M_w = 35,000, M_n = 9000); [10]PEO with M.W. = 1000K g/mol; [11]Lignin (M.W. = 10,000 g/mol, Sigma-Aldrich); [12]Alkali Lignin (M.W. = 60,000 g/mol, Sigma-Aldrich); [13]Poly (vinyl alcohol) (PVA) M.W. = 85K to 124K; [14]PEO with M.W. = 5000K g/mol; [15]N,N-dimethylacetamide; [16]PEO with M.W. = 200K g/mol, [17]PEO with M.W. = 400K g/mol, [18]PZAA@ CNTs: cross-linked polyphosphazene-functionalized carbon nanotubes, [19]PVA with M.W. = 28,000 Da and 31,000–50,000 Da, [20]PVA with M.W = 89,000–98,000, Sigma-Aldrich), [21]PVA with M.W = 145,000–195,000 and PGS: poly(glycerol sebacate), [22]PEO with MW of 1 × 10^6 g/mol and NCCs: nanocrystalline celluloses, [23]KLN, Kraft lignin nanoparticle (particle size ~ 90 nm, Mw = 9000, Sigma-Aldrich, [24]GN, Graphene nanosheet (average thickness < 30 nm, specific surface area ~60 m^2 g^{-1}), [25]Lignin: Alcell Organosolv hardwood lignin, [26]PLA: (3001D), TPU: thermoplastic elastomeric polyurethane, MPI: 7%Methylenediphenyl diisocyanate, [27]rPET: Waste water-bottles were used as the source of PET, [28]Polyacrylonitrile (PAN) with MW 80,000 g/mol, [29]GRP: graphene with an average thickness of 12 nm, [3] PVA with a Mw = 130000 g.mol^{-1} and a degree of hydrolysis of 86–89% was obtained from Sigma-Aldrich under the trade name of Mowiol 18–88, [31]OL: Organosolv Lignin (Lignin, MW = 4000 g mol^{-1}), [32]PVA: Poly(vinyl alcohol) (PVA) (Mw: 30,000–70,000), [33]PVP: Polyvinylpyrrolidone (PVP, Mw = 1,300,000), [34]PEO with MW = 300,000, iron(III) acetylacetonate ($Fe(acac)_3$), (SAN) Poly(styrene-co-acrylonitrile),[35]·t-MWNTs: thin multi-walled carbon nanotubes, [36]PVA with molecular weight of 117,000 and hydrolysis degree of 87–89%, Sigma-Aldrich, [37]PEO: with M.W. = 2000 Kg/mol, [38]Surfactant: Anionic surfactant sodium dodecyl sulfate (SDS), Cationic surfactant N,N,N-trimethyl-1dodecanaminium bromide (DTAB), Nonionic surfactant Triton X-100 (TX-100) from Sigma-Aldrich.

known as carbonization, is to obtain the final carbonized fibers (Ruiz-Rosas et al., 2010b).

Stabilization time is an essential task for industrial carbon fiber production. Depending on the scale of the process, Alcell lignin can take several days (Mainka et al., 2015a). This is due to the devolatilization of lignin which increases the stabilization time. Studies showed that the thermal stabilization of softwood lignin was achieved in a shorter time compared to hardwood lignin (Norberg et al., 2013). However, softwood lignin has lower spinability than hardwood lignin due to the high melting point and cross-linked structure of softwood lignin (Zhang and Ogale, 2014; Cho et al., 2019a). Moreover, studies have shown that lignin fibers containing certain amounts of NaOH or KOH do not require this thermostabilization step. They can be directly carbonized at a low heating rate without having to fuse fibers (Hu and Hsieh, 2013; Poursorkhabi et al., 2016; Schlee et al., 2019a).

Several temperatures and heating rates have been applied for lignin as well as rapid variations in the total oxygen, hydrogen, carbon and mass content above 190°C (Braun et al., 2005). It is proposed that thermal decomposition of lignin starts with hemolytic dissociation of the weakest bond (β-*O*-4 linkage) (Britt et al., 1995, 2000a,b; Fang et al., 2017a). Decomposition continues by a variety of oxidation, rearrangement and elimination reactions initiated by the radicals. Hemolysis of $-OCH_3$ (methoxyl) groups require a slower rate at higher temperatures. The extent and rate of decomposition depend on factors like temperature, heating rate, and oxygen content. Besides hemolysis, autooxidation is an alternative reaction that occurs in the existence of air and forms carbonyl and carboxyl groups on the lignin structure (Fenner and Lephardt, 1981; Braun et al., 2005). For temperatures up to 200–250°C, the formation of carboxyl and carbonyl groups increase the oxygen content of the fiber. At higher temperatures, these functional groups lose oxygen and form anhydrides, esters and crosslinks inside the structures of lignin. At temperatures above 250°C, carbon-carbon aromatic bonds are produced which is suited for stronger materials (Hu and Hsieh, 2013). There is an opposite relation among the glass transition temperature (T_g) and the hydrogen content of lignin. For example, materials with lesser hydrogen content have higher T_g (Braun et al., 2005).

Analysis of evolved gasses during the carbonization of lignin showed that the non-carbon atoms break apart the sample and evolve CO_2, CO and CH_4 gases as well as H_2O (Yang et al., 2007; Ruiz-Rosas et al., 2010b). During carbonization, water molecules are released between 100 and 600°C. The hydroxyl (-OH) groups break at high temperatures, however, the moisture in the samples evolved at lower temperatures ∼100°C. CO_2 is evolved in a temperature range like water desorption. CO is produced in a range from 200 to 800°C resulting from breakage of carbonyl or carboxyl groups or char forming reactions that were dependent on the type of lignin. Chatterjee and Saito (2015) displayed that the content of lignin controlled the char yield and consequently controlled the activated carbon yield. Additionally, the microstructure of char yield depends on the source of biomass and amount of cellulose and lignin. The author showed a reduction in the char yield with increasing low molecular weight fraction of lignin. Releasing of H_2 starts at temperatures above 500°C and reaches to around 700°C. These gases assigned to the volatiles are produced from the reaction of hydrocarbons or depolymerization of phenyl groups (Blanco López et al., 2002; Yang et al., 2007; Ruiz-Rosas et al., 2010b; Foston et al., 2013).

The sample structure is composed primarily of condensed aryl structures at 1000 °C. At temperatures assigned ∼1000°C, the carbonization can sometimes degrade the aryl structures that are produced at lower temperatures (like 800°C) (Foston et al., 2013). Thus, the assembly of the formed carbon fiber depends on the heating condition. The carbonization conditions which are reported in the literature have heating rates of 5 or 10°C/min and maximum temperatures ranging from 600 to 2200°C with residence times at a maximum temperature between 60 and 150 min (Ruiz-Rosas et al., 2010b; Seo et al., 2011; Choi et al., 2013; Dallmeyer et al., 2013; Hu and Hsieh, 2013; Wang et al., 2013; Xu et al., 2013, 2014; Dallmeyer et al., 2014; Hu et al., 2014; Lai et al., 2014a,b; Guo et al., 2015; Schreiber et al., 2015). A recent study showed that the carbonization time of lignin carbon fiber decreased from 708 to 24 min without losing mechanical properties (Bengtsson et al., 2020). Moreover, increasing the carbonization temperature from 600 to 1600°C, improved the modulus from 18 to 77 GPa due to the formation of nanocrystalline graphite (Bengtsson et al., 2020). Most of the literature involves using an inert atmosphere (nitrogen and argon gas). During carbonization, the fibers are free or clamped (Teng et al., 2013) to induce stretching. Stretching of the fiber during thermal treatment by clamp will improve the orientation of the fiber and decrease the fiber diameter consequently enhancing the mechanical properties (tensile modulus < 100 GPa) of the fiber (Reneker and Yarin, 2008).

The yield is calculated according to fiber weight and depends on heating conditions along with the type of lignin. The carbonization conditions applied to electrospun lignin fibers are shown in **Table 2**. Carbonization of lignin fibers is a less energy and time-intensive process (less than 2 h) than the carbonization of PAN fibers (Liu and Kumar, 2012; Baker and Rials, 2013). Bengtsson et al. (2019) showed a reduction in the time required to stabilize lignin fiber from 16 h to less than 2 h at 250°C due to the high carbon content of lignin (60–65%). In the literature, the influences of carbonization temperature on characteristics of carbonized electrospun lignin fibers have been extensively studied (Ruiz-Rosas et al., 2010b; Choi et al., 2013; Dallmeyer et al., 2014; Schreiber et al., 2015). The carbonization temperature has a direct effect on the tensile characteristics of the carbon fiber (Bengtsson et al., 2020). Increasing carbonization temperature led to an enhancement of the tensile modulus, however, decreased elongation at break and reduced fiber diameter. Interestingly, the tensile strength increased till 1000°C and started to decrease above this temperature due to the defect on the fiber at elevated temperature (Bengtsson et al., 2020).

Hollow nano-carbon fibers were shaped by carbonization of Alcell lignin fibers collected from a tri-axial configuration on the three-layer electrospinning (co-electrospinning) (Lallave et al., 2007). Alcell lignin in ethanol solution was the middle layer, glycerine was the core, and ethanol was the outer sheath. The formation of hollow nanocarbon fiber produced

TABLE 2 | Conditions applied to produce carbonized electrospun lignin fibers.

Thermostabilization				Carbonization				Diameter (d) of carbonized fibers	References
Heating rate (°C/min)	**Max. Temp. (°C)**	**Residence time at max. T (h)**	**Purge gas**	**Heating rate (°C/min)**	**Max. Temperature (°C)**	**Residence time at max. T (h)**	**Purge gas**		
0.05	250	2	Air	10	800	2	N_2	Lignin = 348 ± 39 nm CNTs∼347–370 nm	Liu et al., 2020
2	275	1	Air	5	900, 1100	1	N_2	CNFs@50% lignin = 143 nm at 900°C. CNFs@50% lignin = 0.124 nm at 1100°C	Dalton et al., 2019
–	200	3	Air	–	800	1	N_2	–	Meng et al., 2019
0.4	260	1.5	Air	5, 10	1400	1	N_2	–	Dai et al., 2019
0.5	220	8	Air	–	1400	–	N_2	∼140–100 nm @ 800–1400°C	Wei J. et al., 2019
10 °C/min 0.5°C/min	250	15 in		5	900	1	1) Inert 2) CO_2	1) carbonized = 567 nm 2) CO_2-activated = 566 nm	Schlee et al., 2019b
No need for thermostabilizing				3	800	2	5%H_2 in N_2	Range from 163 to 201 nm	Schlee et al., 2019a
0.5	220	8	Air	5	1200	1	Ar	∼200 nm	Ma et al., 2019
–	280	1	Air	5	800	1	Inert gas	370 nm	Yun et al., 2019
1	225	2	Air	2	900	1	N_2	Less than 100 nm	Demiroğlu Mustafov et al., 2019
2.5	250	1	Air	5	550–1200	1	Ar	–	Roman et al., 2019
1	250	–	Air	10	800	1	N_2	20, 40, and 50 wt% lignin is 0.44, 0.41, and 0.3 μm	Zhang et al., 2019
1	250	1	Air	10	900	0.5	N_2	–	Culebras et al., 2019
2	280	1	Air	5	1000	1	N_2	PAN/Lignin (nm), 100/0 ∼291.48, 90/10 ∼184.22, 80/20∼122.45, 70/30∼79.35	Perera Jayawickramage et al., 2019
150 mL/min	200	3	Air	5 mL/h	1000°C.	1	N_2	–	Song et al., 2019
1	350	4	Air	3	800	1	N_2	124–192 nm	Ma et al., 2018
0.2	200	12	N_2	5	1000	0.5	N_2	1007 ± 670 nm	Shi et al., 2018
0.2	250	1	Air	3	900	1	N_2	–	Yu et al., 2018
5	250	1	Air	10	1000	1	N_2	650 nm	Cho et al., 2018
–	–	–	–	2	1000	1	N_2	300 nm	Jia et al., 2018
0.5	200	36	Air	10	600	1.5	N_2	1 μm. 700–900 nm in Fe_3O_4	Lee et al., 2018
5	250	1	Air	5	1500	1	Ar	CNFs-800 = 253 ± 11 CNFs-1000 = 236 ± 18 CNFs-1200 = 225 ± 22 CNFs-1500 = 200 ± 20	Zhao et al., 2018

(Continued)

TABLE 2 | Continued

Thermostabilization				Carbonization				Diameter (d) of carbonized fibers	References
Heating rate (°C/min)	**Max. Temp. (°C)**	**Residence time at max. T (h)**	**Purge gas**	**Heating rate (°C/min)**	**Max. Temperature (°C)**	**Residence time at max. T (h)**	**Purge gas**		
0.5 1	220 280	8 6	Air	5	1200	1	Ar	–	Beck et al., 2017
0.5, 1, 1.5	250	1	Air	5	900	1	Ar	–	Aslanzadeh et al., 2017
1	280	1	aerobic	5	1000	–	N_2	$NiCo_2O_4$@CNF82∼875 nm $NiCo_2O_4$@CNF55∼1830 nm	Lei et al., 2017
0.5	220	6	Air	5	900	1	Ar	–	Fang et al., 2017b
–	250	3	Air	–	1200	1	N_2	150 nm.	Shi et al., 2017
0.08, 0.8	200	100, 1	Air	10	900	–	N_2	600 nm^{-1} μm for CFs, 600 nm^{-3} μm for CFs+H_3PO_4	García-Mateos et al., 2017
–	250	1	Air		1300	–	N_2	200–500 smooth fibrous	Jin et al., 2014
0.25	200	24	Air	10	900	–	N_2	200 nm smooth fibers	Lallave et al., 2007
0.05	200	36	Air	10	1000	–	N_2	–	Ruiz-Rosas et al., 2010b; Berenguer et al., 2015
Cured by E-beam irradiation			N_2	10	1000	1	N_2	–	Seo et al., 2011
1	250	3	Air	10	1000	1	N_2	Half of the precursor fibers	Choi et al., 2013
1	200	2	Air	10	900	2	N_2	∼ 500 nm	Wang et al., 2013
5	250	1	Air	1)* 18.7 2) 10	1000	5 and 1	N_2	∼639 nm with 0% MWNTs ∼579–816 nm with MWNTs	Teng et al., 2013
–	–	–	–	1) 10 2) 10	1000	1 and 2	1) Mix[a] 2) Ar	Outer d = 476 nm, Inner d = 330 nm, Core-shell = 3.5 μm	Xu et al., 2013
–	–	–	–	10	1000	2 then 20 min	1) Mix[a] 2) Ar 3) Mix[b]	–	Xu et al., 2014
Simultaneous thermostabilization and carbonization				1) 10 2) 10	600 or 850	0.5	N_2	With NaOH = 300–500 nm with KOH = 100–300 nm	Hu and Hsieh, 2013; Hu et al., 2014
Range 0.5, 1, 10	220	8	Air	5	1200	1	Ar	Neat PVA: ∼210 nm Lignin/PVA: 100–150 nm	Lai et al., 2014b
5	250	1	Air	–	900	1	Ar	–	Hishida et al., 2009
2	300	2	Air	2	1200	1	N_2	∼250 nm	Schreiber et al., 2015
5	250	1	Air	1) 20 2) 10	1000	1	N_2	634 ± 87 nm	Dallmeyer et al., 2014
–	250	2	–	–	800	2	Ar	800 nm to 1.2 μm	Salas et al., 2014
10	250	2	Air	10	1400	0.5	N_2	∼561.7–739.6 nm	Youe et al., 2015

**Numbers in a single cell show a multi-step process was performed. [a]500 mL/min hydrogen (H_2) and 1 mL/min argon (Ar). [b]Acetylene/argon mixture (100:300 mL/min).*

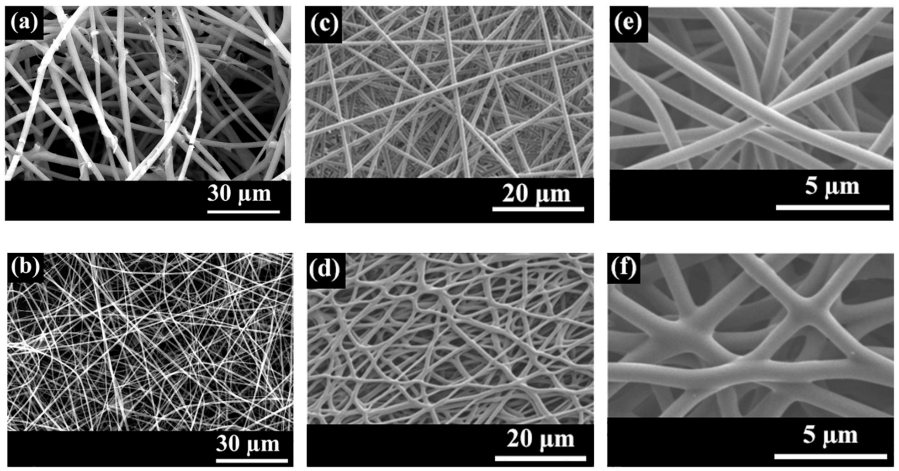

FIGURE 4 | SEM images of softwood kraft lignin electrospun fibers and carbonized fibers. **(a)** fibers from aqueous NaOH solutions of 7% (lignin/PEO: 95/5) (PEO, $M_v = 5 \times 10^6$ g/mol), **(b)** fibers from solution of 11% (lignin/PEO: 95/5) (PEO, Mv = 5×10^6 g/mol) in DMF, **(c)** thermostabilized non-bonded fibers from high molecular weight fraction of lignin and PEO ($M_v = 1 \times 10^6$ g/mol), **(d)** thermostabilized bonded fibers from a 70/30 wt% blend of high and low molecular weight fraction of lignin and PEO ($M_v = 1 \times 10^6$ g/mol), (thermostabilization at 250°C and a heating rate of 5°C/min), **(e,f)** carbonized fibers of **(c,d)** at 1000°C. **(a,b)** Poursorkhabi et al. (2015) (License CC BY-NC-ND, John Wiley and Sons). **(c–f)** Reprinted with permission (Dallmeyer et al., 2014) (License Number 4806541107321), WILEY-VCH Verlag GmbH & Co. KGaA, Weinheim.

fiber with superior mechanical properties and lower weight (Köhler et al., 2017).

The activation of carbon fiber (porous carbon fiber) enhanced the fabrication in different forms and facilitated robust fiber formation. Activated carbon fibers were produced by carbonization of alkaline solutions of PEO/lignin electrospun fibers at 850°C which significantly decreased the impregnation ratio (Hu and Hsieh, 2013). The existence of alkali elements enhanced the shape retention and fiber thermal stability demonstrating that the fibers could be thermostabilized and carbonized in one step under a nitrogen atmosphere.

Multi-walled carbon nanotubes (MWNTs) (Teng et al., 2013) and metal particles such as Platinum (Pt), (Ruiz-Rosas et al., 2010b; Gao et al., 2015). Palladium (Pd) and Gold (Au) (Gao et al., 2015) were also added to the fibers, and their effect on the characteristics of carbonized fibers was investigated. Incorporation of the nanoparticles to lignin carbon fibers improved the mechanical properties, crystallinity of the material and provided further functionality (active phase) as well as value to the material (Beisl et al., 2017; García-Mateos et al., 2019).

CHARACTERIZATION OF THE CARBONIZED FIBERS

Electron Microscopy

Scanning electron microscopy (SEM) is the best technique to evaluate the performance and diameter of fibers. SEM allows one to understand the quality of fibers by characterizing smoothness, roughness or porosity of a fiber surface along with discerning if the surface is non-uniform, beaded, or interconnected (Tagawa and Miyata, 1997; Tanaka et al., 1999; Dallmeyer et al., 2010). Prior to imaging, the electrospun lignin fiber was sputter coated with gold for 10–20 s and examined using accelerating voltages of 5–20 kV. The lignin-carbon fibers formed had a diameter of 80–30 µm. The challenge in decreasing the diameter is restricted by the preparing conditions, for example, clogging melt extrusion die (Kadla et al., 2002; Kadla and Kubo, 2004; Kubo and Kadla, 2004, 2005).

Electrospinning can produce lignin fibers ranging in size from sub-micron to a few micrometers in diameter. The diameter of the lignin fibers depends on multiple variables including type of lignin, solvent, binder polymer; viscosity, concentration, conductivity, surface tension, electrospinning voltage, feed and rate, and the nozzle to collector distance (Huang et al., 2003; Ramakrishna et al., 2005; Dallmeyer et al., 2010). A relatively broad range of diameters has been reported in the literature (Dallmeyer et al., 2010; Teng et al., 2013) and are shown in **Figure 4**.

Figure 4 compares the SEM images of electrospun softwood kraft lignin (MeadWestvaco Indulin-AT, United States) fibers and carbonized fibers. **Figures 4a,b** shows electrospun blend lignin/PEO fibers from aqueous NaOH and DMF solutions, respectively. **Figures 4c–f** demonstrates electrospun fibers from PEO and fractionated lignin and their carbonized fibers. It was observed that enhancing the low-molecular-weight content of lignin increased the chance of fusion of fibers together.

Transmission electron microscopy (TEM) is used to study the fibers surface, strength-structure relationship of the carbon fiber, and dispersion of additives such as metal particles (Ruiz-Rosas et al., 2010b; Lai et al., 2014a) or carbon nanotubes (Teng et al., 2013) in the carbonized fibers. This method is also used to study the carbon structure of the fibers (Hu and Hsieh, 2013; Lai et al., 2014b). The TEM of carbonized samples (powder) were dispersed in ethanol or distilled water by ultrasonic treatment then a droplet was placed on a copper grid supports which was

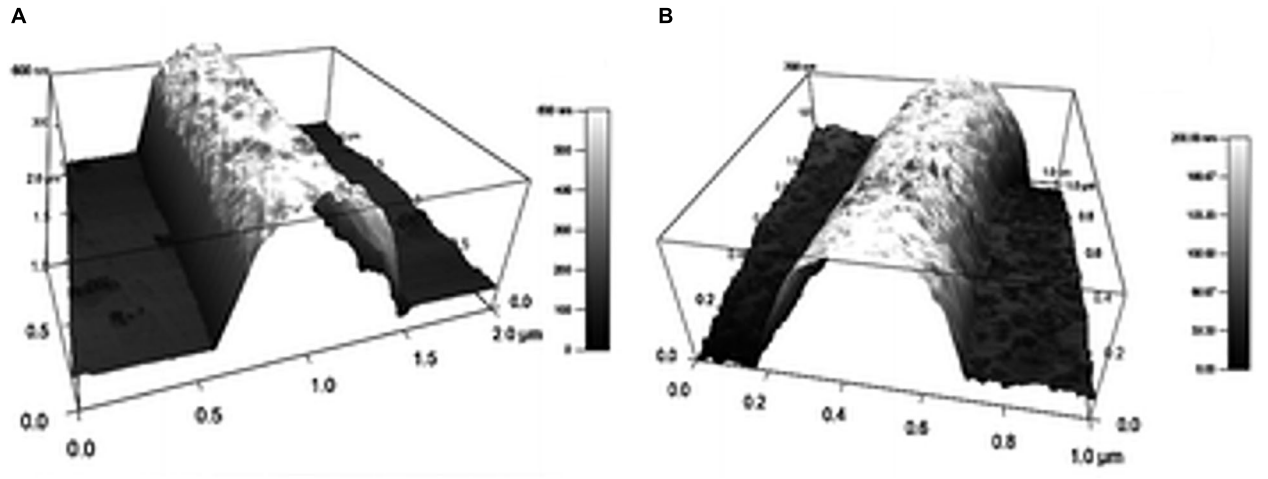

FIGURE 5 | AFM images of activated carbon fibers from blend fibers of (alkali lignin/PEO: 9/1) activated with **(A)** NaOH, and **(B)** KOH. The fibers were carbonized at 850°C for 0.5 h in nitrogen. Reproduced from Hu and Hsieh (2013) with permission from The Royal Society of Chemistry (Order license ID 1029915-1).

then examined by a field emission TEM at an accelerating voltage of ∼100–200 kV. Electrospinning of PAN-lignin fibers displayed a homogeneous circular cross-section with 300 nm diameter at a concentration of 50 wt.% lignin. At 60 wt.% lignin, the formation of beaded fibers occurred and at 80 wt.%, electrospraying had taken place (Seo et al., 2011).

Ruiz-Rosas et al. (2010b) obtained Alcell lignin composite fibers with platinum by co-electrospinning. The fiber diameters were between ∼800 nm and 3 μm. Thermostabilized fibers were not fused and diameters remained in the same range. The maximum deterioration in diameter was between 400 nm and 1 μm after carbonization at the highest temperatures. TEM displayed a smooth surface of the fiber with Pt dispersion of 10.5%.

Hollow carbon fibers have been produced from co-electrospun fibers. In the co-electrospinning process a tri-axial configuration was used. In this configuration, ethanol, lignin solution, and glycerin solution were the outer layer, middle layer, and the inner layer, respectively (Lallave et al., 2007). The fiber was between 400 nm and 2 μm and reduced to 200 nm after carbonization due to the removal of non-carbon compounds, i.e., Oxygen, Hydrogen and Sulfur elements for kraft lignin (Lai et al., 2014b).

Atomic Force Microscopy (AFM)

AFM is used to study the roughness and porosity of the surface of carbon fibers (Hu and Hsieh, 2013). The images obtained from the AFM depends on the shape, size and functionality of the probe tips (Furuno et al., 1998). AFM has different assortment for imaging such as height (smoothness of surface), phase images (sample viscosity and hardness) and amplitude (vibrating the probe) depending on the working environments. The electrospun and carbonized fiber was prepared by fixing the fibers on the surface of cleaved mica and the tip scans over the surface by continuous tapping. **Figure 5** shows AFM images of carbonized (alkali lignin/PEO: 9/1 wt/wt) fibers (Hu and Hsieh, 2013). The fibers were produced from aqueous solutions of NaOH or KOH and carbonized at 850°C for 30 min under a nitrogen blanket. Both images in **Figure 5** demonstrate a porous fiber surface.

Elemental Analysis

CHNS/O analysis is used to measure the degree of carbonization and the percentage of elements in thermally treated lignin fibers (Lallave et al., 2007). The existence of C-O groups has an influence on the solid electrolyte interphase layer forming in the reaction (Choi et al., 2013). Lallave et al. (2007) characterized the percentage of elements in the lignin fibers and thermally treated fibers by elemental analysis. The authors found that thermostabilized fibers have a higher oxygen percentage depending on the temperature and heating rate. Fibers carbonized at 900°C, and above have a carbon content of more than ∼90%.

X-Ray Photoelectron Spectroscopy (XPS and EDX)

XPS and EDX is used as an alternative method for elemental analysis of the fibers (Ruiz-Rosas et al., 2010b; Hu and Hsieh, 2013; Wang et al., 2013). This method was used to investigate the surface chemistry of the samples (Ruiz-Rosas et al., 2010b; Wang et al., 2013).

The surface concentration of oxygen in carbonized fiber (carboxyl, carbonyl, ester, and anhydride groups) increased and the percentage of hydrogen decreased after thermostabilization (in the form CO or CO_2) which resulted in an increase in the T_g of the material (Lallave et al., 2007; Ruiz-Rosas et al., 2010b).

Wang et al. (2013) analyzed the percentage of carbon, nitrogen and oxygen of the carbonized lignin fibers by XPS. The carbonized (lignin/PEO: 90/10) fibers at a 900°C had 89.11% carbon and 10.89% oxygen. The *N*-doped fibers were produced by the second heating of urea impregnated carbon fibers to the 900°C. These fibers had a 76.85% carbon, 9.94% oxygen, and 13.21% nitrogen.

Fourier Transform Infrared Spectroscopy (FTIR)

FTIR is used to detect changes in chemical functionalities after thermostabilization (Hu and Hsieh, 2013; Cho et al., 2019b). It is also used to confirm the complete removal of chemical groups other than carbon in the carbonized fibers (Choi et al., 2013).

Choi et al. (2013) reported producing carbon fibers from lignin/PAN blend fibers. FTIR of the carbonized fibers made from blends of lignin/PAN showed peaks at around 1000 cm^{-1} indicating the presence of C–O groups while the fibers produced only from PAN did not show any significant peak, presenting complete carbonization.

Thermal Analysis

The thermal stability of the electrospun fibers and carbonized fibers up to 1000°C was investigated by thermogravimetric analysis (TGA) in both an air and nitrogen atmosphere (Ruiz-Rosas et al., 2010b; Seo et al., 2011). Non-isothermal oxidation profiles of thermo-stabilized lignin fibers displayed an important oxidation rate at 250°C. Resistance to oxidation of carbonized fibers will be enhanced at higher carbonization temperatures. Lack of superficial defects, as well as ordered carbon, were presented as the causes for higher oxidation onset temperatures (Ruiz-Rosas et al., 2010b). TGA examination of fibers in N_2 atmosphere is used to calculate the carbonization yield as an alternative of direct weight measurements (Lallave et al., 2007; Seo et al., 2011).

Differential scanning calorimetry (DSC) studies are used to determine the transition points of the fibers. DSC results for Lignin/PEO fibers showed the disappearance of the melting point of PEO (Hu and Hsieh, 2013). It is due to a good spreading of PEO in the reinforcing agent (lignin), higher chain entanglement between the two polymers, and the inability of the PEO to crystalize. The other application of DSC is detecting the softening point of the fiber after thermostabilization.

Raman Spectroscopy

Ramen spectroscopy has been used to study the carbon structure of fibers. Raman spectrum of carbonized lignin fibers are displayed as two broad overlapping peaks resulting from disordered carbon with semi-structural organization. The first peak (D band) at ∼1300 cm^{-1} is assigned to carbon hybridization (sp^3) in polycrystalline graphite. It represents the disordered structure, which is called "turbostratic carbon structure" and can constitute the imperfections in the graphitized structure. Another peak (G band) at ∼1576 cm^{-1} because of carbon hybridization (sp^2) as well as stretching mode in the graphite plane (Ferrari and Robertson, 2000). Usually, deconvolution of the Raman spectra peaks are used to measure the intensity and position of each band. The deconvolution of the spectra to two (Choi et al., 2013; Teng et al., 2013; Dallmeyer et al., 2014; Youe et al., 2015), three (Jawhari et al., 1995), or four peaks (Ruiz-Rosas et al., 2010b; Hu et al., 2014; Berenguer et al., 2015) has been reported in the literature. After deconvolution of the spectrum to 4 peaks, two smaller bands at ∼1515 and 1170 cm^{-1} appear. These bands are attributed to impurities such as ions or oxygen superficial groups (Ruiz-Rosas et al., 2010b).

The ratio of intensities of D to G band ($R = I_D/I_G$) is used to study the extent of the ordered graphitic structure. Increasing the *R*-value reveals the enhance in the disordered structure and decreased size of graphite sheets. Crystallite size of graphite (L_α) (nm) and graphitic mole fraction (x_G), can be calculated from Eqs (1) and (2) (Cançado et al., 2006):

$$L_\alpha = (2.4 \times 10^{-10})\lambda^4 \left(\frac{I_D}{I_G}\right)^{-1} \quad (1)$$

Where λ is the incident laser wavelength (nm).

$$x_G = \frac{I_G}{I_D + I_G} = \frac{1}{1 + R} \quad (2)$$

Vicinity of the center of deconvoluted G band to the value for graphite (1582 cm^{-1}) was attributed to the onset of the structural organization although there were still some disordered carbon present (Lallave et al., 2007).

The effects of carbonization temperature were studied with Raman spectroscopy between 600 and 1400°C to calculate the degree of graphitization (Ruiz-Rosas et al., 2010b; Dallmeyer et al., 2014; Liu H.C. et al., 2015; Schreiber et al., 2015; Youe et al., 2015). The results showed that at higher temperatures a narrower G and D band occurred and enhanced the intensity of the G band signal. Increasing the carbonization temperature leads to a decrease in the contribution of the disordered structure of carbonized fibers (Rodríguez-Mirasol et al., 1996; Ruiz-Rosas et al., 2010b). Disordered structure of carbonized fibers which had dispersed metal particles such as platinum or nitrogen-doped fibers increased due to the steric hindrance effect of particles or nitrogen induced defects (Keskar et al., 2005; Ruiz-Rosas et al., 2010b; Wang et al., 2013). Structure of carbonized lignin fibers blended with a crystalline polymer such as cellulose acetate or PVA became more disordered by increasing the content of lignin which has a more amorphous structure (Choi et al., 2013; Lai et al., 2014b; Schreiber et al., 2015).

X-Ray Diffraction (XRD)

The peaks of lignin/PAN fibers at 2θ of 28.8° and 16.8° are due to (110) and (100) crystallographic planes of PAN. These peak intensities decrease after thermostabilization due to variation in the structure of PAN (Seo et al., 2011).

The carbonized lignin shows a broad diffraction peak centered at $2\theta \approx 25–26°$ which is due to (002) crystallographic planes of graphite crystallites (Seo et al., 2011; Teng et al., 2013). For some samples, peaks were detected at around 63.3° and 50.4° assigned to (004) and (100) planes in graphitic structure. The interplanar spacing, d_{002}, of the carbonized fibers improved by increasing the lignin content and reduction of density. Thus, higher lignin content in fiber will lead to the formation of higher porous carbon structures (Lai et al., 2014b). All the lignin-based carbon fibers had a broadband from 15 to 33° due to an amorphous carbon structure.

Surface Area Analysis

Porosity and surface area of the fibers were calculated by N_2 adsorption-desorption at −196°C and application of Brunauer, Emmett, and Teller (BET) equation (Lallave et al., 2007; Ruiz-Rosas et al., 2010b; Wang et al., 2013).

The porosity of the lignin fibers increased during the carbonization process by the removal of volatile material. It was observed that the surface area of carbonized lignin improved from 524 to 1195 m^2/g by increasing the temperature from 600 to 900°C. After a certain temperature, further increasing the temperature to (1000°C) had the opposite effect. It destroyed the porous structure and reduced the surface area (821 m^2/g) due to reorganization of the solid at 1000^{o}C (Ruiz-Rosas et al., 2010b).

Wang et al. (2013) showed a decrease in the surface area from 473 to 381 $m^2.g^{-1}$ of lignin-carbonized fibers doped with nitrogen which resulted in the formation of meso/macro-porous structure.

The pore volume of lignin-carbonized fibers enhanced by increasing the temperature due to the activation by oxygen (activating agent) during carbonization (Ruiz-Rosas et al., 2010b).

The surface area of PAN/lignin-carbonized fibers reduced from 12.9 to 6.3 $m^2.g^{-1}$ with increasing content of lignin, in spite of reduction in diameter due to fiber fusion in the network of the fiber (Choi et al., 2013).

Addition of alkali metal hydroxides such as NaOH or KOH to the lignin solutions traps these materials inside the fibers. Activated carbon fibers were produced from carbonized lignin fibers containing alkali metal compounds (Hu and Hsieh, 2013).

The carbonized lignin-based fibers showed different types of isotherms for porous materials such as types I, II, or IV depending on the fiber composition and carbonization conditions (Ruiz-Rosas et al., 2010b; Hu and Hsieh, 2013; Wang et al., 2013; Lai et al., 2014b). Reversible adsorption was monitored by comparing the desorption and adsorption curves (Ruiz-Rosas et al., 2010b).

Mechanical Properties

Achieving high modulus and strength, lignin carbon fibers require highly oriented anisotropic-graphitic structures along the fiber axis (Davé et al., 1993). Thus, the polymer chains have to be oriented and aligned in one direction before fiber solidification. Fiber diameter also affects the strength. Fibers with a smaller diameter will have less defects and will be molecularly oriented along the fiber axis (Tagawa and Miyata, 1997; Tanaka et al., 1999; Dallmeyer et al., 2010).

Lignin is an amorphous aromatic biopolymer that has a 3D structure. Because of this, molecular orientation is the key to high mechanical properties (modulus and strength) which is limited (Davé et al., 1993). The mechanical characterization of lignin-based carbon fibers were tested using tensile testing machines according to ASTM D638 (Seo et al., 2011; Teng et al., 2013).

Seo et al. (2011) displayed the enhancement of tensile strength of PAN-lignin (50/50) fiber from around ∼100 to more than 800 MPa (around 480%) for fiber irradiated by 2000 KGy dosage compared to PAN-lignin fiber non-irradiated. This is due to stabilization of PAN during irradiation.

Teng et al. (2013) measured the tensile strength of MWNTs dispersed in PEO-lignin carbonized fiber using a micro-tensile tester instrument at rate of 0.02 cm s^{-1}. The tensile strength reduced by inclusion of 1 wt.% MWNTs but stayed equivalent by increasing the concentration. Moreover, the tensile strength decreased by increasing the diameters of the fiber. The strength of PEO-lignin fibers without MWNTs increased from 5.13 to 45.03 MPa after carbonization. The inclusion of 4 wt.% MWNTs decreased the strength to 2.46 MPa due to the poor dispersion. The modulus of PEO-lignin fibers enhanced from 5.1 to 6.2 GPa for carbonized fibers. Incorporation of MWNTs enhanced the modulus but reduced after carbonization from 6.2 to 2.4 GPa due to the change in the morphology of the fibers. The percentage of elongation and toughness reduced after incorporation of MWNTs but the percentage of elongation enhanced after carbonization with no effect on toughness. For carbon fibers, no enhancement was observed by inclusion of MWNTs. It is opposite than the trend observed for PAN, in which addition of MWNTs improved the fiber strength due to the random order of MWNTs in carbon fibers and poor adhesion and dispersion lead to decreasing in the mechanical characteristics.

APPLICATION OF THE CARBONIZED FIBERS

In recent years, the production of carbon fiber from by-product lignin is a key material directly linked to automotive industry, construction aerospace and energy industry (Liu W.-J. et al., 2015; Kai et al., 2016). Energy manufacturing is the fast-growing industry for renewable resource-based alternatives to traditional petroleum-based materials. In particular, supercapacitors, energy storage and dye-synthesized solar cells (DSSCs) are increasingly in demand as the solution to providing low-cost, light-weight, and more energy-efficient devices (Fang et al., 2017a).

Polyacrylonitrile (PAN) is an important precursor material for the production of carbon fiber. However, PAN has a non-renewability and intensive processing conditions as well as a high cost which adds to the product's final cost limiting the application for anode production in batteries (Choi et al., 2013; Wang et al., 2013). Besides lignin, several types of materials have been tested as a potential source of biomass-based carbon such as rice straw (Zhang et al., 2009), bacterial cellulose (Wang et al., 2015), egg protein (Li et al., 2013), sugar (Xing et al., 1996), olive, cherry stones (Caballero et al., 2011), and peanut shells (Fey et al., 2003), etc. However, the disadvantage of these resources is complicated processing (Wang et al., 2013).

Graphene and non-graphene carbons were applied as a major component to produce the electrode for lithium-ion battery anodes (LIBs). This has resulted from their porous structure, processability, availability, chemical stability and low cost (Wang et al., 2013). One of the most important factors for the anode material is to have a high rate capability and high capacity (Choi et al., 2013).

The structural and chemical stability of these materials through Li-ion insertion/de-insertion is the essential property that allows for a reversible charge/discharge process

TABLE 3 | Electrochemical properties of carbonized fibers as lithium-ion battery anodes.

Precursor fiber material used for electrode	Charge/ discharge cycles	Current density ($mA.g^{--1}$)	Initial charge capacity ($mA.h.g^{-1}$)	Initial discharge capacity ($mA.h.g^{-1}$)	Initial columbic efficiency (%)	References
Lignin/PAN: 50/50, 30/70, 0/100	50	37.2	300–310	–	–	Choi et al., 2013
Lignin/PEO: 97/3 Non-interconnected fibers	50	30	365	∼ 650	56.2	Wang et al., 2013
Lignin/PEO: 90/10 Interconnected fibers	50	30	445	∼ 650	68.2	Hishida et al., 2009; Wang et al., 2013
Lignin/PEO: 90/10 Interconnected fibers N-doped	50	30	576	∼ 650	82.8	Wang et al., 2013
Carbonized nanofibers Lignin/PAN: 50/50	400	20	471.0	304.4	64.6	Shi et al., 2017
Mesoporous carbonized nanofibers Lignin/PAN: 50/50	400	20	618.4	384.4	62.2	Shi et al., 2017
Lignin/Cellulose acetate	200	50	290	555	52	Jia et al., 2018
PLA or TPU/Lignin 50/50; 70/30	500	372	611	572	–	Culebras et al., 2019
Lignin/PVA with∼35 wt% Fe_2O_3	80	50, 100, 200	–	∼715	–	Ma et al., 2019
PAN	Second	10, 30, 100	∼450	–	–	Kim et al., 2006
Graphite	second	10, 30, 100	∼320	–	–	Kim et al., 2006

(Choi et al., 2013). Limited theoretical capacity (372 $mA.h.g^{-1}$) and long charging times are limitations of commercial graphite anodes (Choi et al., 2013).

Nano-carbon materials that enhance the rate capability of anodes have high electrical conductivity and large specific surface area (Choi et al., 2013; Wang et al., 2013). Examples of these nano-carbon materials are carbon nanofibers, carbon nanotubes, and graphene. Smaller carbon fiber diameters will lead to higher surface areas as well as better rate capability. Choi et al. (2013) showed that the carbon nanofibers diffusion length of Li-ion is shorter than micro-size graphite materials.

The electrochemical properties of carbonized fibers as lithium-ion battery anodes are summarized in **Table 3**. For fabricating electrodes, carbon nanofibers are blended with other materials as shown in **Table 3**. Choi et al. (2013) made electrodes from lignin carbon nanofibers. They obtained an electrode loading level around 1–2 mg/cm^2 using lithium metal as anode and a polypropylene separator. The fibers from blended lignin/PAN precursors had a smaller surface area. However, the plateau was longer for these fibers due to oxygen groups on the fiber surface. Their results showed that the carbon fibers from lignin/PAN (30/70 and 50/50 wt.%) had a similar rate capability except for initial irreversible capacity. The fibers showed a cycle performance and a high rate compared to traditional PAN fibers.

Wang et al. (2013) fabricated Li-ion batteries by using a carbon fiber mat and a lithium foil as the anode and counter electrode, respectively, made from lignin with different percentages of PEO. The electrical conductivity of interconnected fiber mats was measured at 10.53 S/cm which fared better than separated fiber mats (7.34 S/cm). The charge capacity and electrical conductivity of interconnected fiber mats were enhanced by the incorporation of 12.6 wt% nitrogen to the surface (**Table 3**). The initial discharge curves of carbon fibers showed the plateau corresponding to SEI formation around 1.2 V which disappeared for N-doped carbon fibers. Therefore, SEI formation was hindered by N-doping and the initial capacity loss was reduced.

Dalton et al. (2019) reported that the electrical conductivity of lignin-electrospun CNFs produced at 900 and 1100^{o}C with 70% lignin is 9.65 and 24.47 S/cm, respectively. This enhancement in the electrical conductivity resulted from increasing the degree of graphitization. These new CNF materials with both n-type and p-type semiconducting behaviors can be used in thermoelectric generators.

Zhao et al. (2018) fabricated a new sustainable carbon fiber from lignin/PVA as a highly efficient and binder-free counter electrode for DSSCs. The new electrode of DSSCs has a conversion efficiency of 7.60% which can be used as a substitute to expensive and commercial Pt electrodes (conversion efficiency of 7.67%). García-Mateos et al. (2017) also assembled new Pt-containing carbon fibers which are applied as electrodes with no conductivity promoter or binder.

Various types of carbon materials such as graphene, carbon nanotubes and activated carbon have been reported to manufacture electrodes for supercapacitors. Lignin-carbon fiber has been studied in different publication to manufacture electrodes for capacitors/supercapacitors (Fang et al., 2017b; Lei et al., 2017; Ma et al., 2018; Yu et al., 2018; Perera Jayawickramage et al., 2019; Roman et al., 2019; Schlee et al., 2019a,b; Yun et al., 2019). Lai et al. (2014b) applied lignin-carbon fibers as electrodes to prepare electrochemical supercapacitors as summarized in **Table 4**. The highest gravimetric capacitance was obtained with high alkali lignin content (70%) due to the increase in surface area and decreasing in pore size of fibers. During the test, the electrodes were electrochemically stable or durable.

Figure 6 displayed the cyclic voltametry of lignin/PVA with differernt surfactant which presented largest loop area and superior electrical double-layer capacitive behavior except for carbon fiber with nonionic surfactant Triton X-100 (CNF-TX) (Fang et al., 2017b). CNF with 1.0% anionic surfactant sodium dodecyl sulfate displayed the longest discharge time which resulted in better material capacitance.

TABLE 4 | Electrochemical properties of carbonized fibers as supercapacitor.

Precursor fiber material used for supercapacitor	Gravimetric capacitance ($F\ g^{-1}$)	Energy density ($W\ h\ kg^{-1}$)	Power density ($kW\ kg^{-1}$)	Stability	References
Lignin/Polyvinyl alcohol: 70/30	64 (at 400 mA g^{-1}) 50 (at 2000 mA g^{-1})	5.67	94.19	Dropped 10% after 6000 cycle	Lai et al., 2014b
Lignin/Polyvinyl alcohol/MnO_2	83.3	84.3	5.72		Ma et al., 2016
Lignin/PVA with different surfactant	CNF-C: 66.3 CNF-SDS: 80.7 CNF-DTAB:62.6 CNF-TX: 34	–	–	–	Fang et al., 2017b
$NiCo_2O_4$ oxides-decorated Lignin/PAN	∼1757 (at 2 mA cm^{-2}) 34.3 (at 1 A g^{-1})	47.75	799.53	∼138% capacitance retention after 5000 cycles at 7 mA cm^{-2}	Lei et al., 2017
Lignin/PVP+ $Mg(NO_3)_2{\cdot}6H_2O$ as additive	248 (at 0.2 A g^{-1})	–	–	97% capacitance retention after 1000 cycles at 20 A g^{-1}	Ma et al., 2018
Acetic acid lignin/PEO/ SAN/Iron oxide	121 (at 0.5 A g^{-1})	–	–	90% retention rate after 1000 cycles	Yu et al., 2018
Lignin/PAN (30/70)	128 (at 1 A g^{-1})	59	15	75% retention after 1000 cycles	Perera Jayawickramage et al., 2019
Lignin/PVA	Mat: 7.73 Twist 23 turns/cm: 0.33	–	–	–	Roman et al., 2019
Lignin/PEO	151 without $NaNO_3$, 192 with $NaNO_3$	8.4	60	92.5% retention after 6000 cycles	Schlee et al., 2019a
Lignin non-activated Lignin CO_2-activated	155 (at 0.1 A g^{-1}) 113 (at 250 A g^{-1})	1.2 4	41 52	94% retention after 6000 cycles	Schlee et al., 2019b
PAN/pitch/lignin With ZnO	165 (at 1 mA cm^{-2})	22	0.4	6% reduced after 3000 cycles	Yun et al., 2019

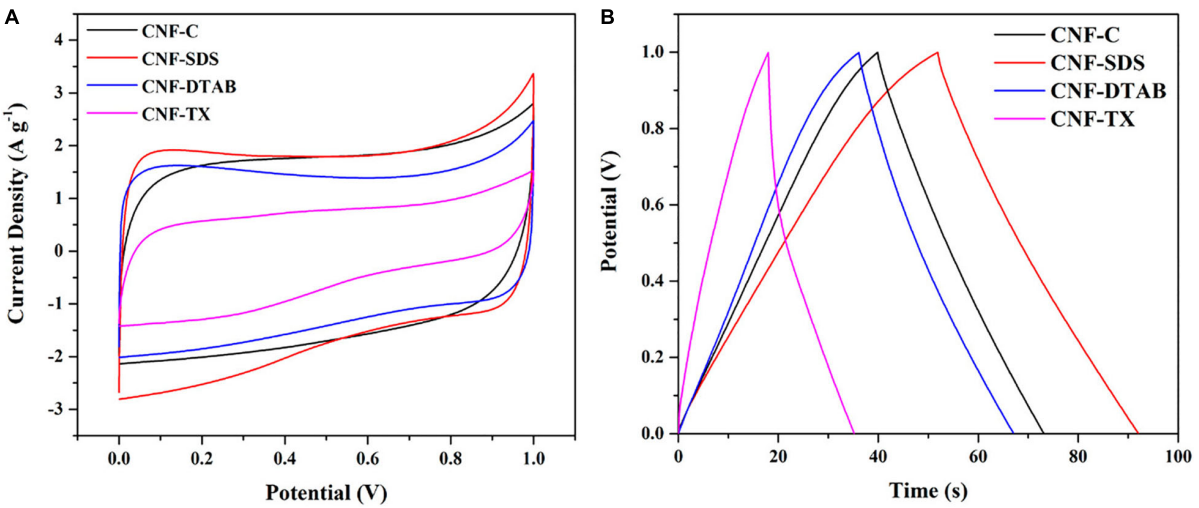

FIGURE 6 | Electrochemical characterizations of carbon fiber membranes from solutions with varying surfactants. **(A)** Cyclic voltammograms curves at 50 mv s^{-1}; **(B)** galvanostatic charge-discharge curves at 1 A g^{-1}. The carbonized mats were labeled as CNF-C, CNF-SDS, CNF-DTAB, and CNF-TX for fibers spun from solutions without surfactant, 1.0% SDS (Anionic surfactant sodium dodecyl sulfate), 1.0% DTAB (Cationic surfactant *N,N,N*-trimethyl-1-dodecanaminium bromide), and 1.0% TX-100 (Nonionic surfactant Triton X-100), respectively. Fang et al. (2017b) with permission from the American Chemical Society.

Due to high surface area, high gas permeability and high porosity, lignin-carbon fiber is applied as an adsorbent for water purification and adsorption of volatile organic compounds (Beck et al., 2017; Song et al., 2017, 2019; Zhang et al., 2019). Zhang et al. (2019) prepared a nanocarbon fiber membrane from Lignin/PVA to adsorb cationic dye (Safranine T). The adsorbent membrane showed superior desorption behavior with the ability to be recycled with constant adsorption performance.

These accomplishments suggest the possible utilization of lignin-carbon fibers for a wide variety of applications, such as supercapacitors, separation, electrodes, catalysis and dye-synthesized solar cells (DSSCs) (Fang et al., 2017a; Zhao et al., 2018; Cao et al., 2020). However, these sustainable materials should be enhanced further especially the mechanical properties and scale-up for industrial commercialization. Recent reviews showed a different technology to scale-up the

electrospinning process for biomedical applications (Vass et al., 2020). The technology of co-axial and multi-axial system offer an opportunity for industrial scale-up of electrospinning.

CONCLUSION

Electrospun fibers have been used as precursors for the production of carbon nanofibers. Electrospinning is a convenient method for the spinning of thermally sensitive biopolymers. This method provides an easy way for the incorporation of metal particles and fillers in the fibers. Additionally, nanofibers have exceptional properties like high surface area and porosity, which is valuable for multiple applications. Due to increasing environmental awareness, renewable resource-based and sustainable materials have been studied as an alternative to the petroleum-based materials. Electrospinning of biopolymer lignin fibers and conversion to carbonized fibers have been studied to develop a convenient process for the production of lignin fibers and carbon fibers. Carbon fibers have been characterized to determine their morphology, physical properties and degree of graphitization. Energy storage devices mainly batteries and supercapacitors have been fabricated by using lignin-based carbon fibers and tested. Promising results have shown these materials have the potential for the next generation of renewable electronics and energy storage devices.

The limitation of lignin-based carbon fiber is the heterogeneity and diversity of lignin which resulted in different characteristic of the fiber produced. By lowering the cost of organosolv lignin, it can be an excellent candidate to overcome this shortage. Another limitation is the necessity of scaling up electrospinning for industrial commercialization, which is the one of the main challenges for electrospinning of polymers. The technology of co-axial and multi-axial system offer an opportunity for industrial scale-up of electrospinning.

The challenge of lignin-based carbon fiber is to apply these fibers in the composite application especially in the automotive industry and in biomedical applications such as facemasks, and shields which are in short supply during global pandemics. Promising results have shown these materials have the potential for the next generation of renewable electronics and energy storage devices. New studies are proceeding to investigate further ways to improve the processing efficiency and determine process-property relationships such as effects of electrospun fiber orientation on the conductivity of the carbonized fibers. These detailed studies will help to further tailor the fiber properties for targeted applications.

AUTHOR CONTRIBUTIONS

All authors listed have made a substantial, direct and intellectual contribution to the work, and approved it for publication.

FUNDING

The authors are thankful for the financial support from the Natural Sciences and Engineering Research Council (NSERC), Canada, for the Discovery grants individual Project # 400320; the Ontario Ministry of Agriculture, Food and Rural Affairs (OMAFRA) – University of Guelph Bioeconomy Industrial Uses Research Program Project # 030332; the Ontario Research Fund, Research Excellence Program; and Round-7 (ORF-RE07) from the Ontario Ministry of Research Innovation and Science (MRIS) (Projects # 052644 and #052665).

REFERENCES

Abdelwahab, M. A., Misra, M., and Mohanty, A. K. (2019). Injection molded biocomposites from polypropylene and lignin: ewffect of compatibilizers on interfacial adhesion and performance. *Ind. Crops Prod.* 132, 497–510. doi: 10.1016/j.indcrop.2019.02.026

Abdelwahab, M. A., Taylor, S., Misra, M., and Mohanty, A. K. (2015). Thermo-mechanical characterization of bioblends from polylactide and poly(butylene adipate-co-terephthalate) and lignin. *Macromol. Mater. Eng.* 300, 299–311. doi: 10.1002/mame.201400241

Achyuthan, K. E., Achyuthan, A. M., Adams, P. D., Dirk, S. M., Harper, J. C., Simmons, B. A., et al. (2010). Supramolecular self-assembled chaos: polyphenolic lignin's barrier to cost-effective lignocellulosic biofuels. *Molecules* 15, 8641–8688. doi: 10.3390/molecules15118641

Adams, B., Abdelwahab, M., Misra, M., and Mohanty, A. K. (2018). Injection-molded bioblends from lignin and biodegradable polymers: processing and performance evaluation. *J. Polym. Environ.* 26, 2360–2373. doi: 10.1007/s10924-017-1132-0

adil, K. R., Mussatto, S. I., and Jha, H. (2018). Synthesis and characterization of silver nanoparticles loaded poly(vinyl alcohol)-lignin electrospun nanofibers and their antimicrobial activity. *Int. J. Biol. Macromol.* 120, 763–767. doi: 10.1016/j.ijbiomac.2018.08.109

Ago, M., Jakes, J. E., Johansson, L.-S., Park, S., and Rojas, O. J. (2012a). Interfacial properties of lignin-based electrospun nanofibers and films reinforced with cellulose nanocrystals. *ACS Appl. Mater. Interfaces* 4, 6849–6856. doi: 10.1021/am302008p

Ago, M., Okajima, K., Jakes, J. E., Park, S., and Rojas, O. J. (2012b). Lignin-based electrospun nanofibers reinforced with cellulose nanocrystals. *Biomacromolecules* 13, 918–926. doi: 10.1021/bm201828g

Ago, M., Jakes, J. E., and Rojas, O. J. (2013). Thermomechanical properties of lignin-based electrospun nanofibers and films reinforced with cellulose nanocrystals: a dynamic mechanical and nanoindentation study. *ACS App. Mater. Interfaces* 5, 11768–11776. doi: 10.1021/am403451w

Ahn, Y., Kang, Y., Park, B., Ku, M. K., Lee, S. H., and Kim, H. (2014). Influence of lignin on rheological behaviors and electrospinning of polysaccharide solution. *J. Appl. Poly. Sci.* 131, 40031–40037. doi: 10.1002/app.40031

Alghoraibi, I., and Alomari, S. (2018). "Different methods for nanofiber design and fabrication," in *Handbook of Nanofibers*, eds A. Barhoum, M. Bechelany, and A. Makhlouf (Cham: Springer International Publishing), 1–46. doi: 10.1007/978-3-319-42789-8_11-2

Aslanzadeh, S., Ahvazi, B., Boluk, Y., and Ayranci, C. (2017). Carbon fiber production from electrospun sulfur free softwood lignin precursors. *J. Eng. Fiber. Fabr.* 12:155892501701200405. doi: 10.1177/155892501701200405

Bahi, A., Shao, J., Mohseni, M., and Ko, F. K. (2017). Membranes based on electrospun lignin-zeolite composite nanofibers. *Sep. Purif. Technol.* 187, 207–213. doi: 10.1016/j.seppur.2017.06.015

Baker, D. A., and Rials, T. G. (2013). Recent advances in low-cost carbon fiber manufacture from lignin. *J. Appl. Polym. Sci.* 130, 713–728. doi: 10.1002/app.39273

Beachley, V., and Wen, X. (2009). Effect of electrospinning parameters on the nanofiber diameter and length. *Mater. Sci. Eng. C* 29, 663–668. doi: 10.1016/j.msec.2008.10.037

Beck, R. J., Zhao, Y., Fong, H., and Menkhaus, T. J. (2017). Electrospun lignin carbon nanofiber membranes with large pores for highly efficient adsorptive water treatment applications. *J. Water Process Eng.* 16, 240–248. doi: 10.1016/j.jwpe.2017.02.002

Beisl, S., Friedl, A., and Miltner, A. (2017). Lignin from micro- to nanosize: applications. *Int. J. Mol. Sci.* 18:2367. doi: 10.3390/ijms18112367

Bengtsson, A., Bengtsson, J., Sedin, M., and Sjöholm, E. (2019). Carbon fibers from lignin-cellulose precursors: effect of stabilization conditions. *ACS Sust. Chem. Eng.* 7, 8440–8448. doi: 10.1021/acssuschemeng.9b00108

Bengtsson, A., Hecht, P., Sommertune, J., Ek, M., Sedin, M., and Sjöholm, E. (2020). Carbon fibers from lignin–cellulose precursors: effect of carbonization conditions. *ACS Sust. Chem. Eng.* 8, 6826–6833. doi: 10.1021/acssuschemeng.0c01734

Berenguer, R., Garcia-Mateos, F. J., Ruiz-Rosas, R., Cazorla-Amoros, D., Morallon, E., Rodriguez-Mirasol, J., et al. (2015). Biomass-derived binderless fibrous carbon electrodes for ultrafast energy storage. *Green Chemi.* 18, 1506–1515. doi: 10.1039/C5GC02409A

Bhardwaj, N., and Kundu, S. C. (2010). Electrospinning: a fascinating fiber fabrication technique. *Biotechnol. Adv.* 28, 325–347. doi: 10.1016/j.biotechadv.2010.01.004

Blanco López, M. C., Blanco, C. G., Martı̀nez-Alonso, A., and Tascón, J. M. D. (2002). Composition of gases released during olive stones pyrolysis. *J. Anal. Appl. Pyrol.* 65, 313–322. doi: 10.1016/S0165-2370(02)00008-6

Braun, J. L., Holtman, K. M., and Kadla, J. F. (2005). Lignin-based carbon fibers: oxidative thermostabilization of kraft lignin. *Carbon* 43, 385–394. doi: 10.1016/j.carbon.2004.09.027

Britt, P. F., Buchanan, A. C. III, and Malcolm, E. A. (1995). Thermolysis of phenethyl phenyl ether: a model for ether linkages in lignin and low rank coal. *J. Org. Chem.* 60, 6523–6536. doi: 10.1021/jo00125a044

Britt, P. F., Buchanan, A. C., Cooney, M. J., and Martineau, D. R. (2000a). Flash vacuum pyrolysis of methoxy-substituted lignin model compounds. *J. Org. Chem.* 65, 1376–1389. doi: 10.1021/jo991479k

Britt, P. F., Buchanan, A. C., and Malcolm, E. A. (2000b). Impact of restricted mass transport on pyrolysis pathways for aryl ether containing lignin model compounds. *Energy Fuels* 14, 1314–1322. doi: 10.1021/ef000160w

Caballero, A., Hernán, L., and Morales, J. (2011). Limitations of disordered carbons obtained from biomass as anodes for real lithium-ion batteries. *ChemSusChem* 4, 658–663. doi: 10.1002/cssc.201000398

Camiré, A., Espinasse, J., Chabot, B., and Lajeunesse, A. (2020). Development of electrospun lignin nanofibers for the adsorption of pharmaceutical contaminants in wastewater. *Environ. Sci. Pollut. Res.* 27, 3560–3573. doi: 10.1007/s11356-018-3333-z

Cançado, L. G., Takai, K., Enoki, T., Endo, M., Kim, Y. A., Mizusaki, H., et al. (2006). General equation for the determination of the crystallite size La of nanographite by Raman spectroscopy. *Appl. Phys. Lett.* 88:163106. doi: 10.1063/1.2196057

Cao, Q., Zhu, M., Chen, J., Song, Y., Li, Y., and Zhou, J. (2020). Novel lignin-cellulose-based carbon nanofibers as high-performance supercapacitors. *ACS Appl. Mater. Interfaces* 12, 1210–1221. doi: 10.1021/acsami.9b14727

Chatterjee, S., and Saito, T. (2015). Lignin-derived advanced carbon materials. *Chem. Eur.* 8, 3941–3958. doi: 10.1002/cssc.201500692

Chen, R., Abdelwahab, M. A., Misra, M., and Mohanty, A. K. (2014). Biobased ternary blends of lignin, poly(Lactic Acid), and Poly(Butylene Adipate-co-Terephthalate): the effect of lignin heterogeneity on blend morphology and compatibility. *J. Polym. Environ.* 22, 439–448. doi: 10.1007/s10924-014-0704-5

Cho, M., Karaaslan, M., Wang, H., and Renneckar, S. (2018). Greener transformation of lignin into ultralight multifunctional materials. *J. f Mater. Chem. A* 6, 20973–20981. doi: 10.1039/C8TA07802E

Cho, M., Karaaslan, M. A., Renneckar, S., and Ko, F. (2017). Enhancement of the mechanical properties of electrospun lignin-based nanofibers by heat treatment. *J. Mater. Sci.* 52, 9602–9614. doi: 10.1007/s10853-017-1160-0

Cho, M., Ko, F. K., and Renneckar, S. (2019a). Impact of thermal oxidative stabilization on the performance of lignin-based carbon nanofiber mats. *ACS Omega* 4, 5345–5355. doi: 10.1021/acsomega.9b00278

Cho, M., Ko, F. K., and Renneckar, S. (2019b). Molecular orientation and organization of technical lignin-based composite nanofibers and films. *Biomacromolecules* 20, 4485–4493. doi: 10.1021/acs.biomac.9b01242

Choi, D., Lee, J.-N., Song, J., Kang, P.-H., Park, J.-K., and Lee, Y. (2013). Fabrication of polyacrylonitrile/lignin-based carbon nanofibers for high-power lithium ion battery anodes. *J. Solid State Electrochem.* 17, 2471–2475. doi: 10.1007/s10008-013-2112-5

Culebras, M., Geaney, H., Beaucamp, A., Upadhyaya, P., Dalton, E., Ryan, K. M., et al. (2019). Bio-derived carbon nanofibres from lignin as high-performance li-ion anode materials. *ChemSusChem* 12, 4516–4521. doi: 10.1002/cssc.201901562

Dai, Z., Ren, P.-G., Jin, Y.-L., Zhang, H., Ren, F., and Zhang, Q. (2019). Nitrogen-sulphur Co-doped graphenes modified electrospun lignin/polyacrylonitrile-based carbon nanofiber as high performance supercapacitor. *J. Power Sour.* 437:226937. doi: 10.1016/j.jpowsour.2019.226937

Dallmeyer, I., Chowdhury, S., and Kadla, J. F. (2013). Preparation and characterization of kraft lignin-based moisture-responsive films with reversible shape-change capability. *Biomacromolecules* 14, 2354–2363. doi: 10.1021/bm400465p

Dallmeyer, I., Ko, F., and Kadla, J. F. (2010). Electrospinning of technical lignins for the production of fibrous networks. *J. Wood Chem. Technol.* 30, 315–329. doi: 10.1080/02773813.2010.527782

Dallmeyer, I., Lin, L. T., Li, Y., Ko, F., and Kadla, J. F. (2014). Preparation and characterization of interconnected, kraft lignin-based carbon fibrous materials by electrospinning. *Macromol. Mater. Eng.* 299, 540–551. doi: 10.1002/mame.201300148

Dalton, N., Lynch, R. P., Collins, M. N., and Culebras, M. (2019). Thermoelectric properties of electrospun carbon nanofibres derived from lignin. *Int. J. Biol. Macromo.* 121, 472–479. doi: 10.1016/j.ijbiomac.2018.10.051

Davé, V., Prasad, A., Marand, H., and Glasser, W. G. (1993). Molecular organization of lignin during carbonization. *Polymer* 34, 3144–3154. doi: 10.1016/0032-3861(93)90382-K

Deitzel, J. M., Kleinmeyer, J., Harris, D., and Beck Tan, N. C. (2001). The effect of processing variables on the morphology of electrospun nanofibers and textiles. *Polymer* 42, 261–272. doi: 10.1016/S0032-3861(00)00250-0

Demiroğlu Mustafov, S., Mohanty, A. K., Misra, M., and . Ö, M. (2019). Fabrication of conductive Lignin/PAN carbon nanofibers with enhanced graphene for the modified electrodes. *Carbon* 147, 262–275. doi: 10.1016/j.carbon.2019.02.058

Dessureault, D. (2014). *Biofuels Annual 2014 – Canada*. Washington, DC: USDA Foreign Agricultural Service.

Fang, W., Yang, S., Wang, X.-L., Yuan, T.-Q., and Sun, R.-C. (2017a). Manufacture and application of lignin-based carbon fibers (LCFs) and lignin-based carbon nanofibers (LCNFs). *Green Chem.* 19, 1794–1827. doi: 10.1039/C6GC03206K

Fang, W., Yang, S., Yuan, T.-Q., Charlton, A., and Sun, R.-C. (2017b). Effects of various surfactants on alkali lignin electrospinning ability and spun fibers. *Ind. Eng. Chem. Res.* 56, 9551–9559. doi: 10.1021/acs.iecr.7b02494

Fenner, R. A., and Lephardt, J. O. (1981). Examination of the thermal decomposition of kraft pine lignin by Fourier transform infrared evolved gas analysis. *J. Agric. Food Chem.* 29, 846–849. doi: 10.1021/jf00106a042

Ferrari, A. C., and Robertson, J. (2000). Interpretation of Raman spectra of disordered and amorphous carbon. *Phys. Rev. B* 61, 14095–14107. doi: 10.1103/physrevb.61.14095

Fey, G. T.-K., Lee, D. C., Lin, Y. Y., and Kumar, T. P. (2003). High-capacity disordered carbons derived from peanut shells as lithium-intercalating anode materials. *Synth. Metals* 139, 71–80. doi: 10.1016/S0379-6779(03)00082-1

Foston, M., Nunnery, G. A., Meng, X., Sun, Q., Baker, F. S., and Ragauskas, A. (2013). NMR a critical tool to study the production of carbon fiber from lignin. *Carbon* 52, 65–73. doi: 10.1016/j.carbon.2012.09.006

Furuno, T., Sasabe, H., and Ikegami, A. (1998). Imaging two-dimensional arrays of soluble proteins by atomic force microscopy in contact mode using a sharp supertip. *Ultramicroscopy* 70, 125–131. doi: 10.1016/S0304-3991(97)00103-4

Gao, G., Ko, F., and Kadla, J. F. (2015). Synthesis of noble monometal and bimetal-modified lignin nanofibers and carbon nanofibers through surface-grafted Poly(2-(Dimethylamino)Ethyl Methacrylate) brushes. *Macromol. Mater. Eng.* 300, 836–847. doi: 10.1002/mame.201500006

García-Mateos, F. J., Berenguer, R., Valero-Romero, M. J., Rodríguez-Mirasol, J., and Cordero, T. (2018). Phosphorus functionalization for the rapid preparation of highly nanoporous submicron-diameter carbon fibers by electrospinning of lignin solutions. *J. Materi. Chem. A* 6, 1219–1233. doi: 10.1039/C7TA08788H

García-Mateos, F. J., Cordero-Lanzac, T., Berenguer, R., Morallón, E., Cazorla-Amorós, D., Rodríguez-Mirasol, J., et al. (2017). Lignin-derived Pt supported

carbon (submicron)fiber electrocatalysts for alcohol electro-oxidation. *Appl. Catal. BEnviron.* 211, 18–30. doi: 10.1016/j.apcatb.2017.04.008

García-Mateos, F. J., Ruiz-Rosas, R., Rosas, J. M., Rodríguez-Mirasol, J., and Cordero, T. (2019). Controlling the composition, morphology, porosity, and surface chemistry of lignin-based electrospun carbon materials. *Front. Mater.* 6:114. doi: 10.3389/fmats.2019.00114

Guo, Z., Liu, Z., Ye, L., Ge, K., and Zhao, T. (2015). The production of lignin-phenol-formaldehyde resin derived carbon fibers stabilized by BN preceramic polymer. *Mater. Lett.* 142, 49–51. doi: 10.1016/j.matlet.2014.11.068

Han, D., and Steckl, A. J. (2019). Coaxial electrospinning formation of complex polymer fibers and their applications. *ChemPlusChem* 84, 1453–1497. doi: 10.1002/cplu.201900281

Hatakeyama, H., and Hatakeyama, T. (2010). Lignin structure. Properties and applications. *Adv. Polym. Sci.* 232, 1–63. doi: 10.1007/12_2009_12

Hishida, M., Shikinaka, K., Inazawa, M., Katayama, Y., Kajita, S., Masai, E., et al. (2009). Conductive cements based polyesters of PDC(2-Pyrone-4,6-Dicarboxylic Acid) obtained from a metabolic intermediate of lignin. *Kobunshi Ronbunshu* 66, 141–146. doi: 10.1295/koron.66.141

Hu, S., and Hsieh, Y.-L. (2013). Ultrafine microporous and mesoporous activated carbon fibers from alkali lignin. *J. Mater. Chem. A* 1, 11279–11288. doi: 10.1039/C3TA12538F

Hu, S., Zhang, S., Pan, N., and Hsieh, Y.-L. (2014). High energy density supercapacitors from lignin derived submicron activated carbon fibers in aqueous electrolytes. *J. Power Sour.* 270, 106–112. doi: 10.1016/j.jpowsour.2014.07.063

Huang, Z.-M., Zhang, Y. Z., Kotaki, M., and Ramakrishna, S. (2003). A review on polymer nanofibers by electrospinning and their applications in nanocomposites. *Compos. Sci. Technol.* 63, 2223–2253. doi: 10.1016/S0266-3538(03)00178-7

Inagaki, M., Yang, Y., and Kang, F. (2012). carbon nanofibers prepared via electrospinning. *Adv. Mater.* 24, 2547–2566. doi: 10.1002/adma.201104940

Jawhari, T., Roid, A., and Casado, J. (1995). Raman spectroscopic characterization of some commercially available carbon black materials. *Carbon* 33, 1561–1565. doi: 10.1016/0008-6223(95)00117-V

Jia, H., Sun, N., Dirican, M., Li, Y., Chen, C., Zhu, P., et al. (2018). Electrospun kraft lignin/cellulose acetate-derived nanocarbon network as an anode for high-performance sodium-ion batteries. *ACS Appl. Mater. Interfaces* 10, 44368–44375. doi: 10.1021/acsami.8b13033

Jin, J., Yu, B.-J., Shi, Z.-Q., Wang, C.-Y., and Chong, C.-B. (2014). Lignin-based electrospun carbon nanofibrous webs as free-standing and binder-free electrodes for sodium ion batteries. *J. Power Sour.* 272, 800–807. doi: 10.1016/j.jpowsour.2014.08.119

Kadla, J. F., and Kubo, S. (2003). Miscibility and hydrogen bonding in blends of poly(ethylene oxide) and kraft lignin. *Macromolecules* 36, 7803–7811. doi: 10.1021/ma0348371

Kadla, J. F., and Kubo, S. (2004). Lignin-based polymer blends: analysis of intermolecular interactions in lignin–synthetic polymer blends. *Compos. Part AAppl. Sci. Manufactur.* 35, 395–400. doi: 10.1016/j.compositesa.2003.09.019

Kadla, J. F., Kubo, S., Venditti, R. A., Gilbert, R. D., Compere, A. L., and Griffith, W. (2002). Lignin-based carbon fibers for composite fiber applications. *Carbon* 40, 2913–2920. doi: 10.1016/S0008-6223(02)00248-8

Kai, D., Tan, M. J., Chee, P. L., Chua, Y. K., Yap, Y. L., and Loh, X. J. (2016). Towards lignin-based functional materials in a sustainable world. *Green Chemistry* 18, 1175–1200. doi: 10.1039/C5GC02616D

Keskar, G., Rao, R., Luo, J., Hudson, J., Chen, J., and Rao, A. M. (2005). Growth, nitrogen doping and characterization of isolated single-wall carbon nanotubes using liquid precursors. *Chem. Phys. Lett.* 412, 269–273. doi: 10.1016/j.cplett.2005.07.007

Kim, C., Yang, K. S., Kojima, M., Yoshida, K., Kim, Y. J., Kim, Y. A., et al. (2006). Fabrication of electrospinning-derived carbon nanofiber webs for the anode material of lithium-ion secondary batteries. *Adv. Funct. Mater.* 16, 2393–2397. doi: 10.1002/adfm.200500911

Köhler, T., Brüll, R., Pursche, F., Langgartner, J., Seide, G., and Gries, T. (2017). High strength and low weight hollow carbon fibres. *IOP Conf. Ser. Mater. Sci. Eng.* 254:042017. doi: 10.1088/1757-899x/254/4/042017

Kubo, S., and Kadla, J. F. (2004). Poly(Ethylene Oxide)/Organosolv lignin blends: relationship between thermal properties. *Chem. Struct. Blend Beha. Macromol.* 37, 6904–6911. doi: 10.1021/ma0490552

Kubo, S., and Kadla, J. F. (2005). Lignin-based carbon fibers: effect of synthetic polymer blending on fiber properties. *J. Polym. Environ.* 13, 97–105. doi: 10.1007/s10924-005-2941-0

Kubo, S., and Kadla, J. F. (2006). Effect of poly(ethylene oxide) molecular mass on miscibility and hydrogen bonding with lignin. *Holzforschung* 60, 245–252. doi: 10.1515/hf.2006.040

Kumar, M., Hietala, M., and Oksman, K. (2019). Lignin-Based electrospun carbon nanofibers. *Front. Mater.* 6:62. doi: 10.3389/fmats.2019.00062

Kumar, M. N. S., Mohanty, A. K., Erickson, L., and Misra, M. (2009). Lignin and its applications with polymers. *J. Biobased Mater. Bioener.* 3, 1–24. doi: 10.1166/jbmb.2009.1001

Kumar, P. R., Khan, N., Vivekanandhan, S., Satyanarayana, N., Mohanty, A. K., and Misra, M. (2012). Nanofibers: effective generation by electrospinning and their applications. *J. Nanosci. Nanotechnol.* 12, 1–25. doi: 10.1166/jnn.2012.5111

Lai, C., Kolla, P., Zhao, Y., Fong, H., and Smirnova, A. L. (2014a). Lignin-derived electrospun carbon nanofiber mats with supercritically deposited Ag nanoparticles for oxygen reduction reaction in alkaline fuel cells. *Electrochim. Acta* 130, 431–438. doi: 10.1016/j.electacta.2014.03.006

Lai, C., Zhou, Z., Zhang, L., Wang, X., Zhou, Q., Zhao, Y., et al. (2014b). Free-standing and mechanically flexible mats consisting of electrospun carbon nanofibers made from a natural product of alkali lignin as binder-free electrodes for high-performance supercapacitors. *J. Power Sour.* 247, 134–141. doi: 10.1016/j.jpowsour.2013.08.082

Lallave, M., Bedia, J., Ruiz-Rosas, R., Rodrí-guez-Mirasol, J., Cordero, T., Otero, J. C., et al. (2007). Filled and hollow carbon nanofibers by coaxial electrospinning of alcell lignin without binder polymers. *Adv. Mater.* 19, 4292–4296. doi: 10.1002/adma.200700963

Laurichesse, S., and Avérous, L. (2014). Chemical modification of lignins: towards biobased polymers. *Prog. Polym. Sci. Top. Issue Biomater.* 39, 1266–1290. doi: 10.1016/j.progpolymsci.2013.11.004

Lee, E.-S., Kim, Y.-O., Ha, Y.-M., Lim, D., Hwang, J. Y., Kim, J., et al. (2018). Antimicrobial properties of lignin-decorated thin multi-walled carbon nanotubes in poly(vinyl alcohol) nanocomposites. *Eur. Poly. J.* 105, 79–84. doi: 10.1016/j.eurpolymj.2018.05.014

Lei, D., Li, X.-D., Seo, M.-K., Khil, M.-S., Kim, H.-Y., and Kim, B.-S. (2017). NiCo2O4 nanostructure-decorated PAN/lignin based carbon nanofiber electrodes with excellent cyclability for flexible hybrid supercapacitors. *Polymer* 132, 31–40. doi: 10.1016/j.polymer.2017.10.051

Li, X., Chen, Y., Huang, H., Mai, Y.-W., and Zhou, L. (2016). Electrospun carbon-based nanostructured electrodes for advanced energy storage – A review. *Energy Storage Mater.* 5, 58–92. doi: 10.1016/j.ensm.2016.06.002

Li, Z., Xu, Z., Tan, X., Wang, H., Holt, C. M. B., Stephenson, T., et al. (2013). Mesoporous nitrogen-rich carbons derived from protein for ultra-high capacity battery anodes and supercapacitors. *Energy Environ. Sci.* 6, 871–878. doi: 10.1039/C2EE23599D

Li, Z., and Wang, C. (eds). (2013). "Effects of working parameters on electrospinning," in *One-Dimensional Nanostructures: Electrospinning Technique and Unique Nanofibers* (Berlin: Springer Berlin Heidelberg), 15–28. doi: 10.1007/978-3-642-36427-3_2

Liu, H. C., Chien, A.-T., Newcomb, B. A., Liu, Y., and Kumar, S. (2015). Processing, Structure, and properties of lignin- and CNT-Incorporated polyacrylonitrile-based carbon fibers. *ACS Sust. Chem. Eng.* 3, 1943–1954. doi: 10.1021/acssuschemeng.5b00562

Liu, W.-J., Jiang, H., and Yu, H.-Q. (2015). Thermochemical conversion of lignin to functional materials: a review and future directions. *Green Chem.* 17, 4888–4907. doi: 10.1039/C5GC01054C

Liu, S., Cheng, X., He, Z., Liu, J., Zhang, X., Xu, J., et al. (2020). Amine-terminated highly cross-linked polyphosphazene-functionalized carbon nanotube-reinforced lignin-based electrospun carbon nanofibers. *ACS Sust. Chem. Eng.* 8, 1840–1849. doi: 10.1021/acssuschemeng.9b05940

Liu, Y., and Kumar, S. (2012). Recent progress in fabrication. Structure, and properties of carbon fibers. *Polym. Rev.* 52, 234–258. doi: 10.1080/15583724.2012.705410

Lora, J. H., and Glasser, W. G. (2002). Recent industrial applications of lignin: a sustainable alternative to nonrenewable materials. *J. Polym. Environ.* 10, 39–48. doi: 10.1023/A:1021070006895

Ma, X., Kolla, P., Zhao, Y., Smirnova, A. L., and Fong, H. (2016). Electrospun lignin-derived carbon nanofiber mats surface-decorated with MnO_2

nanowhiskers as binder-free supercapacitor electrodes with high performance. *J. Power Sources* 325, 541–548. doi: 10.1016/j.jpowsour.2016.06.073

Ma, C., Li, Z., Li, J., Fan, Q., Wu, L., Shi, J., et al. (2018). Lignin-based hierarchical porous carbon nanofiber films with superior performance in supercapacitors. *Appl. Surface Sci.* 456, 568–576. doi: 10.1016/j.apsusc.2018.06.189

Ma, X., Smirnova, A. L., and Fong, H. (2019). Flexible lignin-derived carbon nanofiber substrates functionalized with iron (III) oxide nanoparticles as lithium-ion battery anodes. *Mater. Sci. Eng. B* 241, 100–104. doi: 10.1016/j.mseb.2019.02.013

Mainka, H., Hilfert, L., Busse, S., Edelmann, F., Haak, E., and Herrmann, A. S. (2015a). Characterization of the major reactions during conversion of lignin to carbon fiber. *J. Mater. Res. Technol.* 4, 377–391. doi: 10.1016/j.jmrt.2015.04.005

Mainka, H., Täger, O., Körner, E., Hilfert, L., Busse, S., Edelmann, F. T., et al. (2015b). Lignin – an alternative precursor for sustainable and cost-effective automotive carbon fiber. *J. Mater. Res. Techno.* 4, 283–296. doi: 10.1016/j.jmrt.2015.03.004

Meng, F., Song, M., Wei, Y., and Wang, Y. (2019). The contribution of oxygen-containing functional groups to the gas-phase adsorption of volatile organic compounds with different polarities onto lignin-derived activated carbon fibers. *Environ. Sci. Pollut. Res.* 26, 7195–7204. doi: 10.1007/s11356-019-04190-6

Mohanty, A. K., Vivekanandhan, S., Pin, J.-M., and Misra, M. (2018). Composites from renewable and sustainable resources: challenges and innovations. *Science* 362, 536–542. doi: 10.1126/science.aat9072

Norberg, I., Nordström, Y., Drougge, R., Gellerstedt, G., and Sjöholm, E. (2013). A new method for stabilizing softwood kraft lignin fibers for carbon fiber production. *Appl. Polym.* 128, 3824–3830. doi: 10.1002/app.38588

Oroumei, A., Fox, B., and Naebe, M. (2015). Thermal and rheological characteristics of biobased carbon fiber precursor derived from low molecular weight organosolv Lignin. *ACS Sust. Chem. Eng.* 3, 758–769. doi: 10.1021/acssuschemeng.5b00097

Perera Jayawickramage, R. A., Balkus, K. J., and Ferraris, J. P. (2019). Binder free carbon nanofiber electrodes derived from polyacrylonitrile-lignin blends for high performance supercapacitors. *Nanotechnology* 30:355402. doi: 10.1088/1361-6528/ab2274

Persano, L., Camposeo, A., Tekmen, C., and Pisignano, D. (2013). Industrial upscaling of electrospinning and applications of polymer nanofibers: a review. *Macromol. Mater. Eng.* 298, 504–520. doi: 10.1002/mame.201200290

Poursorkhabi, V. (2016). *Production and Evaluation of Carbonized Electrospun Fibers from Bioethanol Lignin*. Ph.D. Thesis, University of Guelph, Guelph, ON.

Poursorkhabi, V., Misra, M., and Mohanty, A. K. (2013). Extraction of lignin from a coproduct of the cellulosic ethanol industry and its thermal characterization. *BioResources* 8, 5083–5101.

Poursorkhabi, V., Mohanty, A. K., and Misra, M. (2015). Electrospinning of aqueous lignin/poly(ethylene oxide) complexes. *J. Appl. Polym. Sci.* 132:41260. doi: 10.1002/app.41260

Poursorkhabi, V., Mohanty, A. K., and Misra, M. (2016). Statistical analysis of the effects of carbonization parameters on the structure of carbonized electrospun organosolv lignin fibers. *J. Appl. Polym. Sci.* 133, 44005–44022. doi: 10.1002/app.44005

Prabu, G. T. V., and Dhurai, B. (2020). A novel profiled multi-pin electrospinning system for nanofiber production and encapsulation of nanoparticles into nanofibers. *Sci. Rep.* 10:4302. doi: 10.1038/s41598-020-60752-6

Ramakrishna, S., Fujihara, K., Teo, W. E., Lim, T. C., and Ma, Z. (2005). *An Introduction to Electrospinning and Nanofibers*. Singapore: World Scientific Publishing Co. Pte. Ltd.

Reneker, D. H., and Yarin, A. L. (2008). Electrospinning jets and polymer nanofibers. *Polymer* 49, 2387–2425. doi: 10.1016/j.polymer.2008.02.002

Reneker, D. H., Yarin, A. L., Fong, H., and Koombhongse, S. (2000). Bending instability of electrically charged liquid jets of polymer solutions in electrospinning. *J. Appl. Phys.* 87, 4531–4547. doi: 10.1063/1.373532

Rodríguez-Mirasol, J., Cordero, T., and Rodríguez, J. J. (1996). High-temperature carbons from kraft lignin. *Carbon* 34, 43–52. doi: 10.1016/0008-6223(95)00133-6

Roman, J., Neri, W., Derré, A., and Poulin, P. (2019). Electrospun lignin-based twisted carbon nanofibers for potential microelectrodes applications. *Carbon* 145, 556–564. doi: 10.1016/j.carbon.2019.01.036

Ruiz-Rosas, R., Bedia, J., Lallave, M., Barrero, A., Loscertales, I. G., Rodríguez-Mirasol, J., et al. (2010a). "Preparation and characterization of co-electrospun lignin/alumina microfibers and tubes," in *Carbon, International Carbon Conference*, Clemson, CA: American Carbon Society.

Ruiz-Rosas, R., Bedia, J., Lallave, M., Loscertales, I. G., Barrero, A., Rodrßguez-Mirasol, J., et al. (2010b). The production of submicron diameter carbon fibers by the electrospinning of lignin. *Carbon* 48, 696–705. doi: 10.1016/j.carbon.2009.10.014

Saito, T., Brown, R. H., Hunt, M. A., Pickel, D. L., Pickel, J. M., Messman, J. M., et al. (2012). Turning renewable resources into value-added polymer: development of lignin-based thermoplastic. *Green Chem.* 14, 3295–3303. doi: 10.1039/C2GC35933B

Salas, C., Ago, M., Lucia, L. A., and Rojas, O. J. (2014). Synthesis of soy protein–lignin nanofibers by solution electrospinning. *React. Funct. Polym.* 85, 221–227. doi: 10.1016/j.reactfunctpolym.2014.09.022

Saudi, A., Amini, S., Amirpour, N., Kazemi, M., Zargar Kharazi, A., Salehi, H., et al. (2019). Promoting neural cell proliferation and differentiation by incorporating lignin into electrospun poly(vinyl alcohol) and poly(glycerol sebacate) fibers. *Mater. Sci. Eng. C* 104:110005. doi: 10.1016/j.msec.2019.110005

Sauer, M. (2019). "Composites Market Report 2019", in *Carbon Composites*. Frankfurt: AVK.

Schlee, P., Herou, S., Jervis, R., Shearing, P. R., Brett, D. J. L., Baker, D., et al. (2019a). Free-standing supercapacitors from Kraft lignin nanofibers with remarkable volumetric energy density. *Chem. Sci.* 10, 2980–2988. doi: 10.1039/C8SC04936J

Schlee, P., Hosseinaei, O., Baker, D., Landmér, A., Tomani, P., Mostazo-López, M. J., et al. (2019b). From waste to wealth: from kraft lignin to free-standing supercapacitors. *Carbon* 145, 470–480. doi: 10.1016/j.carbon.2019.01.035

Schreiber, M., Vivekanandhan, S., Cooke, P., Mohanty, A., and Misra, M. (2014). Electrospun green fibres from lignin and chitosan: a novel polycomplexation process for the production of lignin-based fibres. *J. Mater. Sci.* 49, 7949–7958. doi: 10.1007/s10853-014-8481-z

Schreiber, M., Vivekanandhan, S., Mohanty, A. K., and Misra, M. (2012). A Study on the electrospinning behaviour and nanofibre morphology of anionically charged lignin. *Adv. Mater. Lett.* 4, 476–480. doi: 10.5185/amlett.2012.icnano.336

Schreiber, M., Vivekanandhan, S., Mohanty, A. K., and Misra, M. (2015). Iodine treatment of lignin-cellulose acetate electrospun fibres: enhancement of green fibre carbonization. *ACS Sust. Chem. Eng.* 3, 33–41. doi: 10.1021/sc500481k

Seo, D. K., Jeun, J. P., Kim, H. B., and Kang, P. H. (2011). Preparation and characterization of the carbon nanofiber mat produced from electrospun PAN/lignin precursors by electron beam irradiation. *Rev. Adv. Mater. Sci.* 28, 31–34.

Shi, X., Wang, X., Tang, B., Dai, Z., Chen, K., and Zhou, J. (2018). Impact of lignin extraction methods on microstructure and mechanical properties of lignin-based carbon fibers. *J. Appl. Polym. Sci.* 135:45580. doi: 10.1002/app.45580

Shi, Z., Jin, G., Wang, J., and Zhang, J. (2017). Free-standing, welded mesoporous carbon nanofibers as anode for high-rate performance Li-ion batteries. *J. Electroanal. Chem.* 795, 26–31. doi: 10.1016/j.jelechem.2017.03.047

Solomon, B. D., Barnes, J. R., and Halvorsen, K. E. (2007). Grain and cellulosic ethanol: history, economics, and energy policy. *Biomass Bioenergy* 31, 416–425. doi: 10.1016/j.biombioe.2007.01.023

Song, M., Yu, L., Song, B., Meng, F., and Tang, X. (2019). Alkali promoted the adsorption of toluene by adjusting the surface properties of lignin-derived carbon fibers. *Environ. Sci. Pollut. Res.* 26, 22284–22294. doi: 10.1007/s11356-019-05456-9

Song, M., Zhang, W., Chen, Y., Luo, J., and Crittenden, J. C. (2017). The preparation and performance of lignin-based activated carbon fiber adsorbents for treating gaseous streams. *Front. Chem. Sci. Eng.* 11:328–337. doi: 10.1007/s11705-017-1646-y

Suhas, A., Carrott, P. J. M., and Carrott, M. M. L. R. (2007). Lignin – from natural adsorbent to activated carbon: a review. *Bioresour. Technol.* 98, 2301–2312. doi: 10.1016/j.biortech.2006.08.008

Svinterikos, E., and Zuburtikudis, I. (2017). Tailor-made electrospun nanofibers of biowaste lignin/recycled Poly(Ethylene Terephthalate). *J. Polym. he Environ.* 25, 465–478. doi: 10.1007/s10924-016-0806-3

Svinterikos, E., Zuburtikudis, I., and Al-Marzouqi, M. (2019). The nanoscale dimension determines the carbonization outcome of electrospun lignin/recycled-PET fibers. *Chem. Eng. Sci.* 202, 26–35. doi: 10.1016/j.ces.2019.03.013

Tagawa, T., and Miyata, T. (1997). Size effect on tensile strength of carbon fibers. *Mater. Sci. Eng. A* 238, 336–342. doi: 10.1016/S0921-5093(97)00454-1

Tan, S., Huang, X., and Wu, B. (2007). Some fascinating phenomena in electrospinning processes and applications of electrospun nanofibers. *Polym. Int.* 56, 1330–1339. doi: 10.1002/pi.2354

Tanaka, T., Nakayama, H., Sakaida, A., and Horikawa, N. (1999). Estimation of tensile strength distribution for carbon fiber with diameter variation along fiber. *J. Soc. Mater. Sci. Jpn.* 48, 90–97. doi: 10.2472/jsms.48.6Appendix_90

Teng, N.-Y., Dallmeyer, I., and Kadla, J. F. (2013). Incorporation of multiwalled carbon nanotubes into electrospun softwood kraft lignin-based fibers. *J. Wood Chem. Technol.* 33, 299–316. doi: 10.1080/02773813.2013.795807

Teo, W.-E., Inai, R., and Ramakrishna, S. (2011). Technological advances in electrospinning of nanofibers. *Sci. Technol. Adv. Mater.* 12, 1–19.

Thompson, C. J., Chase, G. G., Yarin, A. L., and Reneker, D. H. (2007). Effects of parameters on nanofiber diameter determined from electrospinning model. *Polymer* 48, 6913–6922. doi: 10.1016/j.polymer.2007.09.017

Vass, P., Szabó, E., Domokos, A., Hirsch, E., Galata, D., Farkas, B., et al. (2020). Scale-up of electrospinning technology: applications in the pharmaceutical industry. *Wiley Interdiscip. Rev.* 12:e1611. doi: 10.1002/wnan.1611

Wang, S.-X., Yang, L., Stubbs, L. P., Li, X., and He, C. (2013). Lignin-derived fused electrospun carbon fibrous mats as high performance anode materials for lithium ion batteries. *ACS Appl. Mater. Interfaces* 5, 12275–12282. doi: 10.1021/am4043867

Wang, W., Sun, Y., Liu, B., Wang, S., and Cao, M. (2015). Porous carbon nanofiber webs derived from bacterial cellulose as an anode for high performance lithium ion batteries. *Carbon* 91, 56–65. doi: 10.1016/j.carbon.2015.04.041

Wei, J., Geng, S., Kumar, M., Pitkänen, O., Hietala, M., and Oksman, K. (2019). Investigation of structure and chemical composition of carbon nanofibers developed from renewable precursor. *Front. Mater.* 6:334. doi: 10.3389/fmats.2019.00334

Wei, L., Sun, R., Liu, C., Xiong, J., and Qin, X. (2019). Mass production of nanofibers from needleless electrospinning by a novel annular spinneret. *Mater. Des.* 179:107885. doi: 10.1016/j.matdes.2019.107885

Xing, W., Xue, J. S., and Dahn, J. R. (1996). Optimizing pyrolysis of sugar carbons for use as anode materials in lithium-ion batteries. *J. Electrochem. Soc.* 143, 3046–3052. doi: 10.1149/1.1837162

Xu, X., Zhou, J., Jiang, L., Lubineau, G., Chen, Y., Wu, X.-F., et al. (2013). Porous core-shell carbon fibers derived from lignin and cellulose nanofibrils. *Mater. Lett.* 109, 175–178. doi: 10.1016/j.matlet.2013.07.082

Xu, X., Zhou, J., Jiang, L., Lubineau, G., Payne, S. A., and Gutschmidt, D. (2014). Lignin-based carbon fibers: carbon nanotube decoration and superior thermal stability. *Carbon* 80, 91–102. doi: 10.1016/j.carbon.2014.08.042

Yang, H., Yan, R., Chen, H., Lee, D. H., and Zheng, C. (2007). Characteristics of hemicellulose, cellulose and lignin pyrolysis. *Fuel* 86, 1781–1788. doi: 10.1016/j.fuel.2006.12.013

Yoo, S. H., Park, S., Park, Y., Lee, D., Joh, H.-I., Shin, I., et al. (2017). Facile method to fabricate carbon fibers from textile-grade polyacrylonitrile fibers based on electron-beam irradiation and its effect on the subsequent thermal stabilization process. *Carbon* 118, 106–113. doi: 10.1016/j.carbon.2017.03.039

Youe, W.-J., Lee, S.-M., Lee, S.-S., Lee, S.-H., and Kim, Y. S. (2015). Characterization of carbon nanofiber mats produced from electrospun lignin-g-polyacrylonitrile copolymer. *Int. J. Biol. Macromol.* 82, 497–504. doi: 10.1016/j.ijbiomac.2015.10.022

Yu, B., Gele, A., and Wang, L. (2018). Iron oxide/lignin-based hollow carbon nanofibers nanocomposite as an application electrode materials for supercapacitors. *Int. J. Biol. Macromol.* 118, 478–484. doi: 10.1016/j.ijbiomac.2018.06.088

Yun, S. I., Kim, S. H., Kim, D. W., Kim, Y. A., and Kim, B.-H. (2019). Facile preparation and capacitive properties of low-cost carbon nanofibers with ZnO derived from lignin and pitch as supercapacitor electrodes. *Carbon* 149, 637–645. doi: 10.1016/j.carbon.2019.04.105

Zeng, Y., Zhao, S., Yang, S., and Ding, S.-Y. (2014). Lignin plays a negative role in the biochemical process for producing lignocellulosic biofuels. *Curr. Opin. Biotechnol.* 27, 38–45. doi: 10.1016/j.copbio.2013.09.008

Zhang, B., Kang, F., Tarascon, J.-M., and Kim, J.-K. (2016). Recent advances in electrospun carbon nanofibers and their application in electrochemical energy storage. *Prog. Mater. Sci.* 76, 319–380. doi: 10.1016/j.pmatsci.2015.08.002

Zhang, F., Wang, K.-X., Li, G.-D., and Chen, J.-S. (2009). Hierarchical porous carbon derived from rice straw for lithium ion batteries with high-rate performance. *Electrochem. Commun.* 11, 130–133. doi: 10.1016/j.elecom.2008.10.041

Zhang, M., and Ogale, A. A. (2014). Carbon fibers from dry-spinning of acetylated softwood kraft lignin. *Carbon* 69, 626–629. doi: 10.1016/j.carbon.2013.12.015

Zhang, W., Yang, P., Li, X., Zhu, Z., Chen, M., and Zhou, X. (2019). Electrospun lignin-based composite nanofiber membrane as high-performance absorbent for water purification. *Int. J. Biol. Macromol.* 141, 747–755. doi: 10.1016/j.ijbiomac.2019.08.221

Zhao, L., and Wang, D. (2020). Combined effects of a biobutanol/ethanol–gasoline (E10) blend and exhaust gas recirculation on performance and pollutant emissions. *ACS Omega* 5, 3250–3257. doi: 10.1021/acsomega.9b03303

Zhao, Y., Liu, Y., Tong, C., Ru, J., Geng, B., Ma, Z., et al. (2018). Flexible lignin-derived electrospun carbon nanofiber mats as a highly efficient and binder-free counter electrode for dye-sensitized solar cells. *J. Mater. Sci.* 53, 7637–7647. doi: 10.1007/s10853-018-2059-0

Conflict of Interest: The authors declare that this review article has been designed and written in collaboration with the industry partner HK, The Woodbridge Group. The Woodbridge Group has no financial interests in this article.